Combining texture, structure, microstructure and phase analyses for multiphase bulks and thin films diffraction characterisation: some case studies

Daniel Chateigner, Sandrine Miro, Jacques Noudem
CRISMAT-ENSICAEN (Caen-France)
Magali Morales
SIFCOM-ENSICAEN (Caen-France)
Emmanuel Guilmeau
LSIC (Liege-Belgium)
Jesus Ricote
DMF-ICMM (Madrid-España)
Bachir Ouladdiaf
ILL (Grenoble-France)
Luca Lutterotti
DIM (Trento-Italia)

Bi2223 Superconductors

Irradiated FAp ceramics

$Ca_3Co_4O_9$ Thermoelectrics

PCT Ferroelectrics

nano-Si thin films

Genf 2005

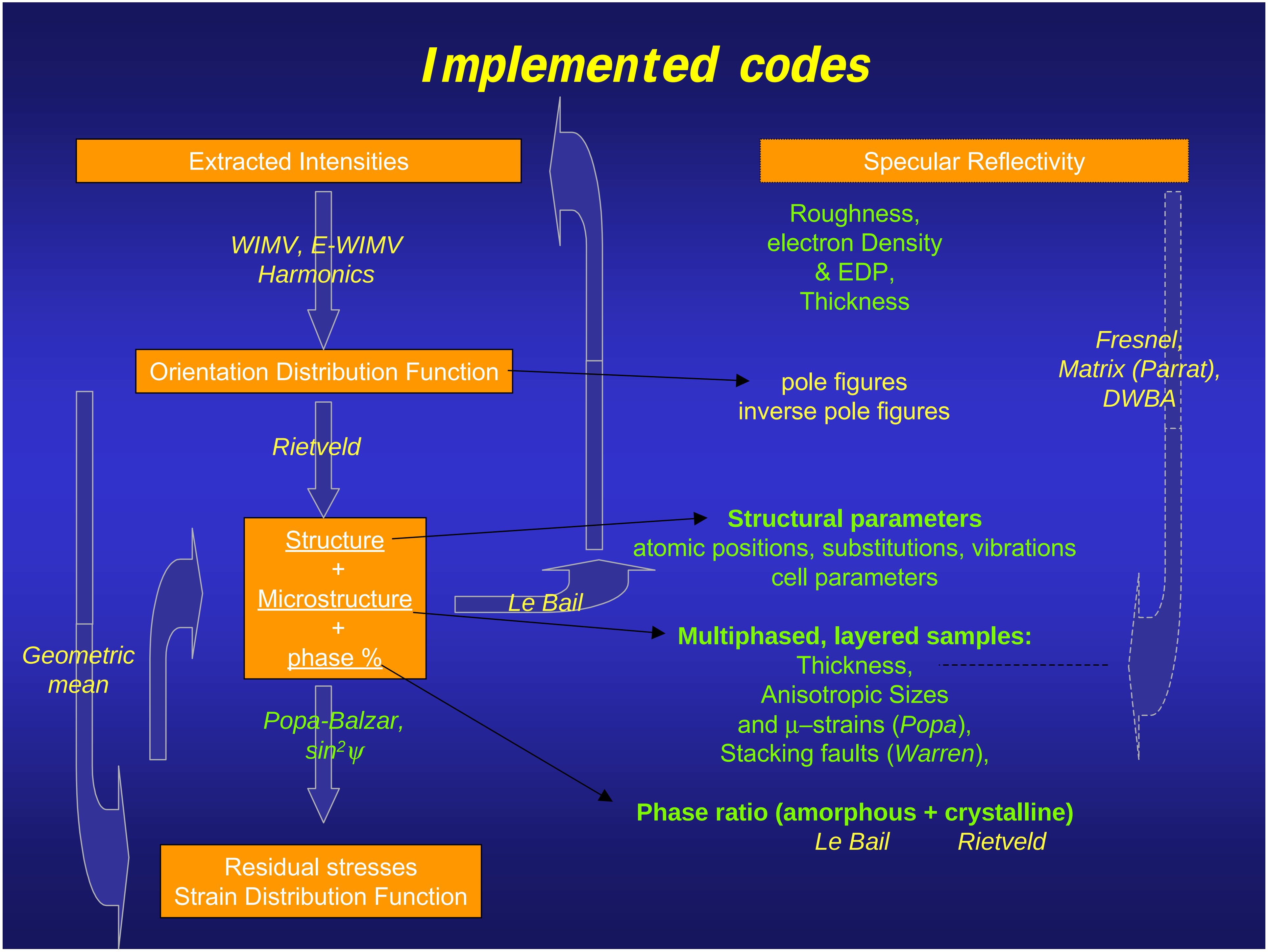
Implemented codes
Extracted Intensities
WIMV, E-WIMV
Harmonics
Orientation Distribution Function
Rietveld
Structure
+
Microstructure
+
phase %
Geometric
mean
Popa-Balzar,
sin²ψ
Residual stresses
Strain Distribution Function
Le Bail
Specular Reflectivity
Roughness,
electron Density
& EDP,
Thickness
Fresnel,
Matrix (Parrat),
DWBA
pole figures
inverse pole figures
Structural parameters
atomic positions, substitutions, vibrations
cell parameters
Multiphased, layered samples:
Thickness,
Anisotropic Sizes
and μ–strains (Popa),
Stacking faults (Warren),
Phase ratio (amorphous + crystalline)
Le Bail
Rietveld

Texture from Spectra

Orientation Distribution Function (ODF)

From pole figures

From spectra

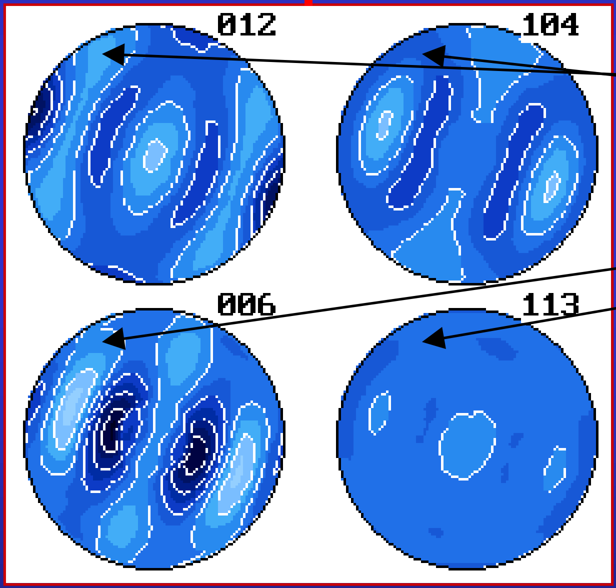

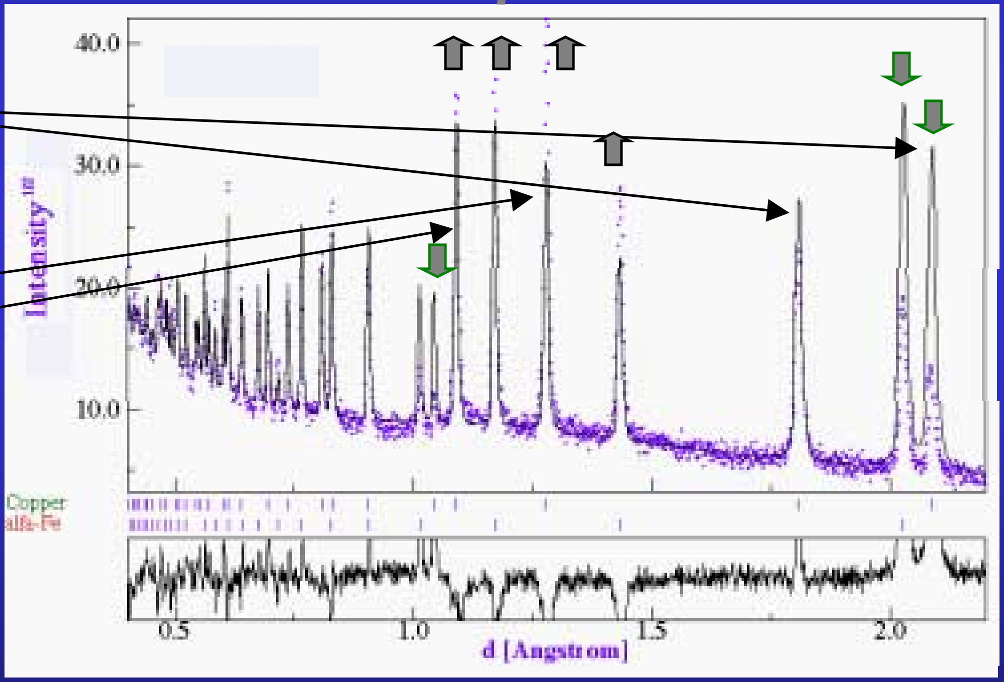

Residual Stresses and Rietveld

- Macro elastic strain tensor (I kind)
- Crystal anisotropic strains (II kind)

C

Macro and micro stresses

Applied macro stresses

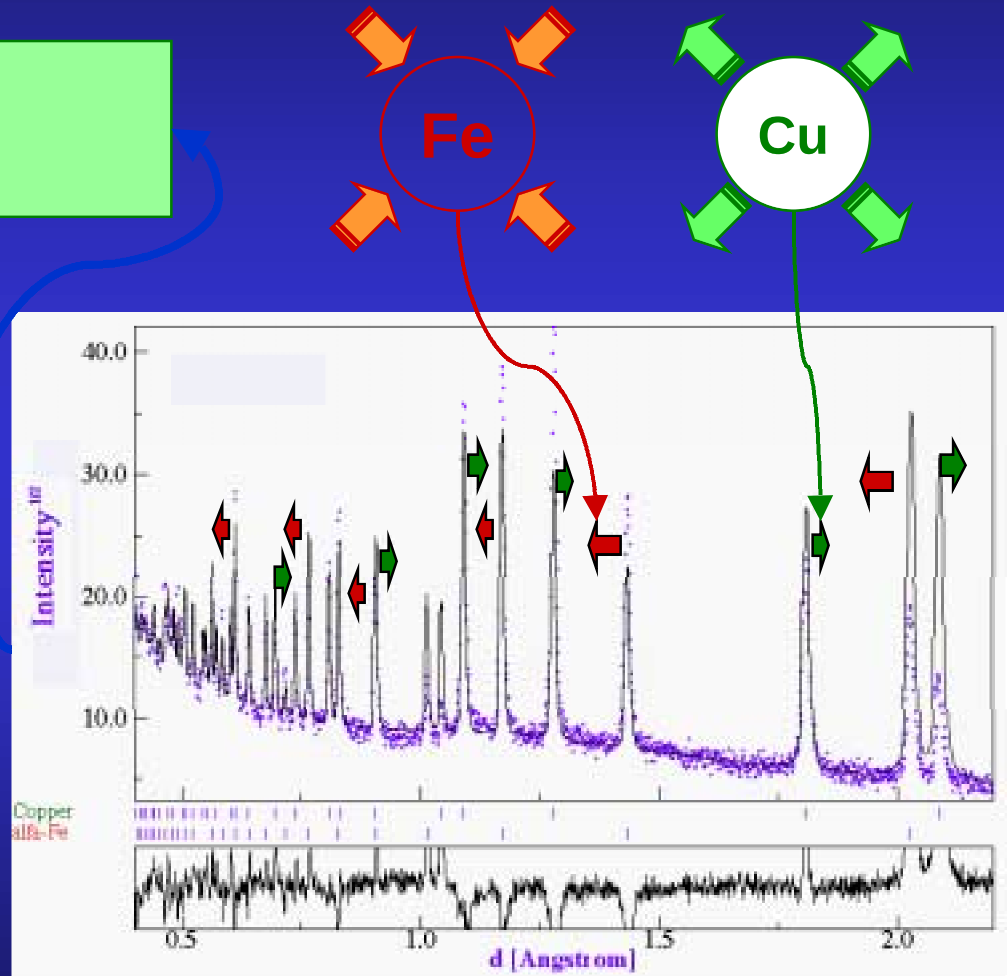

Textured samples: Reuss, Voigt, Hill, Bulk geometric mean approaches

How it works (Combined)

$$I_i^{calc}(\chi,\phi) = \sum_{n=1}^{Nphases} S_n \sum_k L_k \left|F_{k;n}\right|^2 S(2\theta_i - 2\theta_{k;n}) P_{k;n}(\chi,\phi) A + bkg_i$$

Texture

$$P_k(\chi,\phi) = \int_{\varphi} f(g,\varphi) d\varphi$$

- from Generalized Spherical Harmonics:

$$P_k(\chi,\phi) = \sum_{l=0}^{\infty} \frac{1}{2l+1} \sum_{n=-l}^{l} k_l^n(\chi,\phi) \sum_{m=-l}^{l} C_l^{mn} k_n^{*m}(\Theta_k \phi_k)$$

$$f(g) = \sum_{l=0}^{\infty} \sum_{m,n=-l}^{l} C_l^{mn} T_l^{mn}(g)$$

- from the WIMV (left) iterative process or entropy maximisation (right):

$$f^{n+1}(g) = N_n \frac{f^n(g) f^0(g)}{\left(\prod_{\mathbf{h}=1}^{I} \prod_{m=1}^{M_\mathbf{h}} P_\mathbf{h}^n(\mathbf{y}) \right)^{\frac{1}{IM_\mathbf{h}}}}$$

$$f^{n+1}(g) = f^n(g) \prod_{m=1}^{M_\mathbf{h}} \left(\frac{P_\mathbf{h}(\mathbf{y})}{P_\mathbf{h}^n(\mathbf{y})} \right)^{\frac{r_\mathbf{n}}{M_\mathbf{h}}}$$

Layering

$$C_\chi^{\text{top film}} = g_1\left(1-\exp\left(-\mu T g_2/\cos\chi\right)\right)/\left(1-\exp\left(-2\mu T/\sin\omega\cos\chi\right)\right)$$

$$C_\chi^{\text{cov. layer}} = C_\chi^{\text{top film}}\left(\exp\left(-g_2\sum\mu_i^{'}T_i^{'}/\cos\chi\right)\right)/\left(\exp\left(-2\sum\mu_i^{'}T_i^{'}/\sin\omega\cos\chi\right)\right)$$

Popa anisotropic shapes & microstrains

$$\langle R_{\mathbf{h}}\rangle = R_0 + R_1P_2^0(x) + R_2P_2^1(x)\cos\varphi + R_3P_2^1(x)\sin\varphi + R_4P_2^2(x)\cos2\varphi + R_5P_2^2(x)\sin2\varphi + \ldots$$

$$\langle\varepsilon_{\mathbf{h}}^2\rangle E_{\mathbf{h}}^4 = E_1h^4 + E_2k^4 + E_3\ell^4 + 2E_4h^2k^2 + 2E_5\ell^2k^2 + 2E_6h^2\ell^2 + 4E_7h^3k + 4E_8h^3\ell + 4E_9k^3h + 4E_{10}k^3\ell + 4E_{11}\ell^3h + 4E_{12}\ell^3k + 4E_{13}h^2k\ell + 4E_{14}k^2h\ell + 4E_{15}\ell^2kh$$

Roughness and/or microabsorption

$$R^{rough}(q_z) = R(q_z)\exp(-q_{z,0}q_{z,1}\sigma^2)$$ Low-angles (reflectivity)

$$S_R = 1-p\exp(-q)+p\exp\left(\frac{-q}{\sin\theta}\right)$$ high-angle (Suortti)

Specular reflectivity: **q**=(0,0,z)

- Fresnel:

$$R(\mathbf{q}) = \left| \frac{q_z - \sqrt{q_z^2 - q_c^2 + \frac{32 i \pi^2 \beta}{\lambda^2}}}{q_z + \sqrt{q_z^2 - q_c^2 + \frac{32 i \pi^2 \beta}{\lambda^2}}} \right|^2 \delta q_x \delta q$$

- matrix:

$$R^{flat} = \frac{r_{0,1}^2 + r_{1,2}^2 + 2 r_{0,1} r_{1,2} \cos 2 k_{Z,1} h}{1 + r_{0,1}^2 r_{1,2}^2 + 2 r_{0,1} r_{1,2} \cos 2 k_{Z,1} h}$$

- Born approximation:

$$R(q_z) = r.r^* = R_F(q_z) \left| \frac{1}{\rho_s} \int_{-\infty}^{+\infty} \frac{d\rho(z)}{dz} e^{i q_z z} dz \right|^2$$

Phase

$$W_\Phi = \frac{S_\Phi Z_\Phi M_\Phi V_\Phi}{\sum_{i=1}^{N_\Phi} S_i Z_i M_i V_i}$$

Strain-Stress

$$\boldsymbol{\varepsilon}(\mathbf{X}) = \boldsymbol{\varepsilon}^{\mathrm{I}} + \boldsymbol{\varepsilon}^{\mathrm{II}}(\mathbf{X}) + \boldsymbol{\varepsilon}^{\mathrm{III}}(\mathbf{X})$$

$$\begin{aligned}
\langle \varepsilon_{h}(y) \rangle_{V_d} &= \frac{1}{V_d} \int_{V_d} (\varepsilon_{33}^{I} + \varepsilon_{33}^{II} + \varepsilon_{33}^{III}) dV \\
&= (\varepsilon_{11}^{I} \cos^2\phi + \varepsilon_{12}^{I} \sin 2\phi + \varepsilon_{22}^{I} \sin^2\phi - \varepsilon_{33}^{I}) \sin^2\psi + \varepsilon_{33}^{I} + \\
&\quad (\varepsilon_{13}^{I} \cos\phi + \varepsilon_{23}^{I} \sin\phi) \sin 2\psi + \frac{1}{V_d} \int_{V_d} (\varepsilon_{33}^{IIe} + \varepsilon_{33}^{IIti} + \varepsilon_{33}^{IIpi}) dV \\
&= \frac{\langle d(hkl,\phi,\psi) \rangle_{V_d} - d_0(hkl)}{d_0(hkl)}
\end{aligned}$$

Isotropic samples:
triaxial, biaxial uniaxial stress state

Textured samples:
triaxial, biaxial uniaxial stress state
+ ODF + SDF + model

$$\begin{aligned}
\langle E(g) \rangle_{V_d} &= \frac{1}{V_d} \int_{V_d} E^{SC}(g) f(g) dg \\
&= \left(\prod_{V_d} E^{SC}(g) f(g) dg \right)^{\frac{1}{V_d}}
\end{aligned}$$

Reuss, Voigt, Hill

Geometric mean

Minimum experimental requirements

1D or 2D Detector + 4-circle diffractometer
(X-rays and neutrons)
CRISMAT, ILL

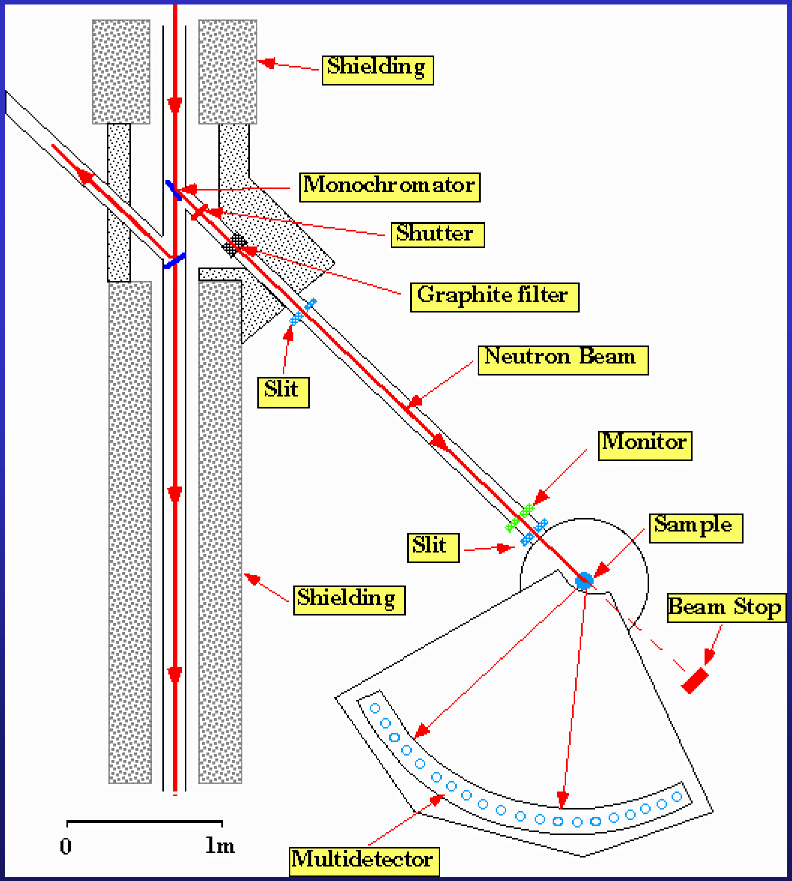

+

~1000 experiments (2θ diagrams)
in as many sample orientations

+

Instrument calibration
(peaks widths and shapes,
misalignments, defocusing …)

Calibration

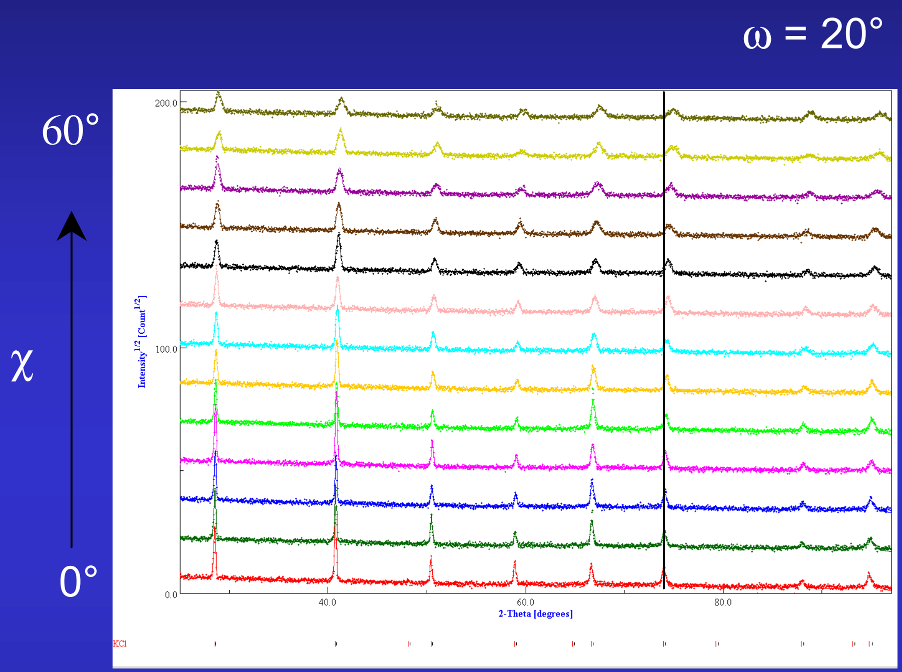

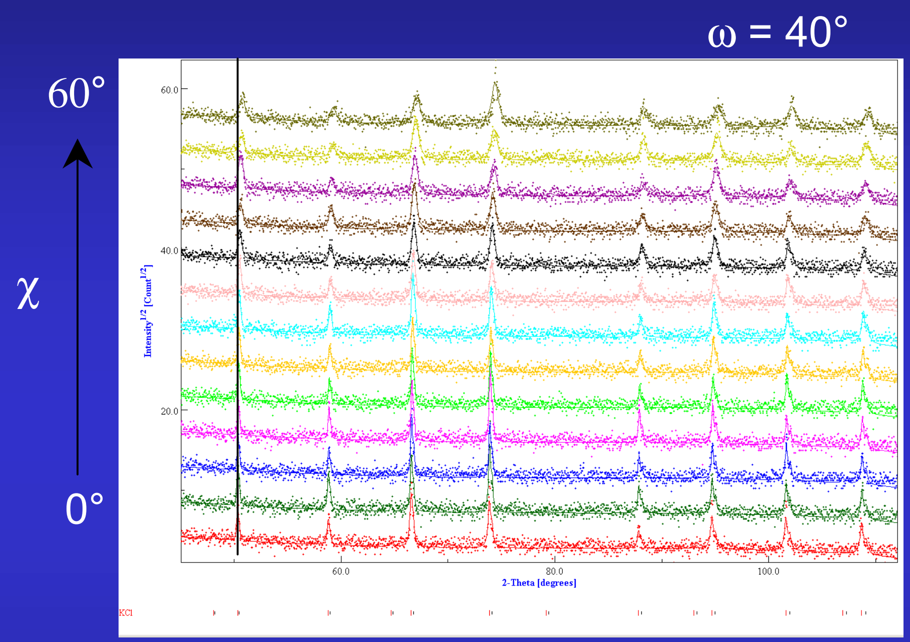

KCl, LaB_6 …

FWHM (ω, χ, 2θ …)
2θ shift
gaussianity
asymmetry
misalignments ...

Methodology implementation

L. Lutterotti, Trento

User friendly interface

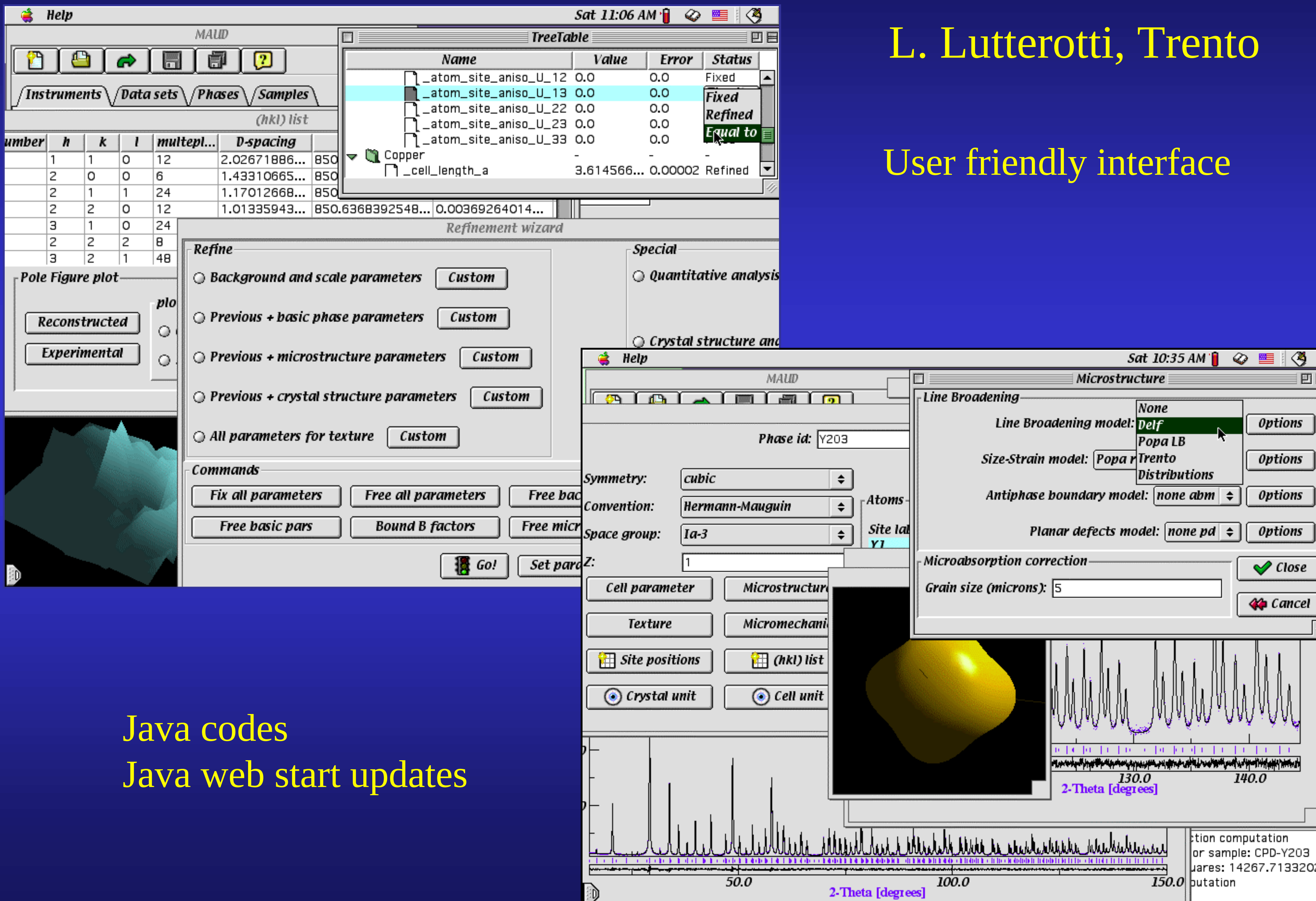

Java codes

Java web start updates

Bi2223 compounds

E. Guilmeau, PhD

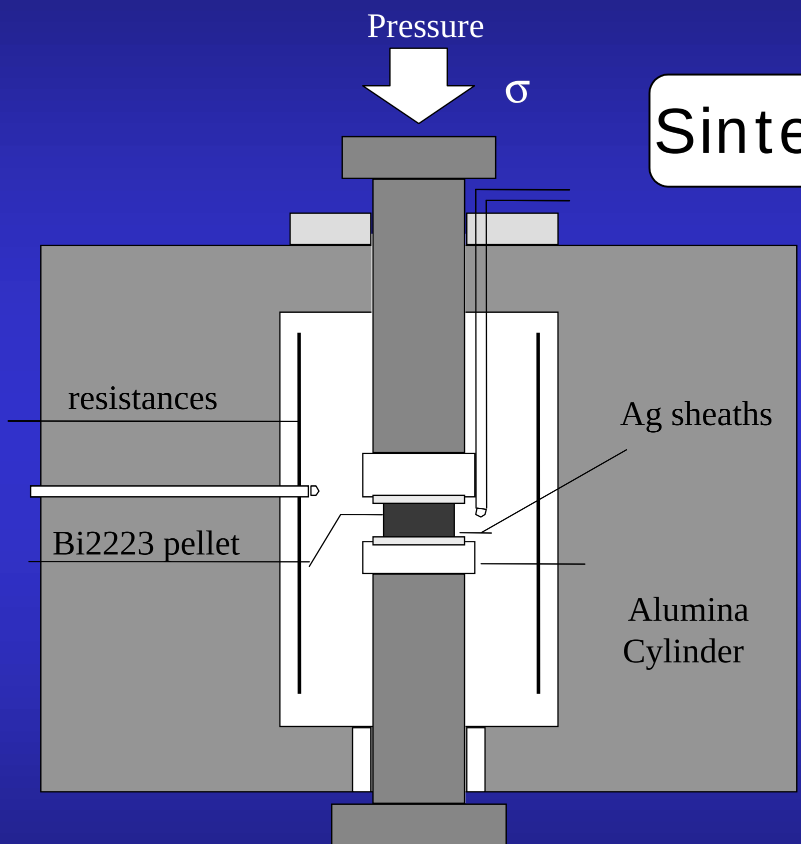

Sinter-Forging

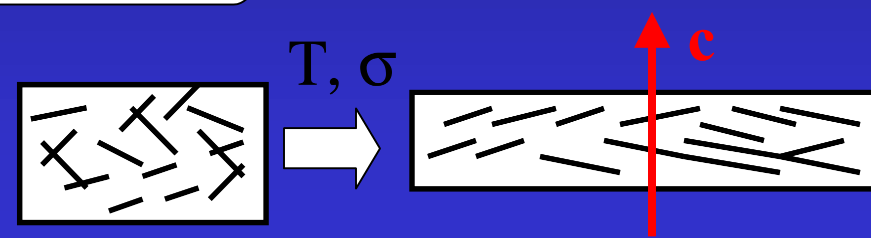

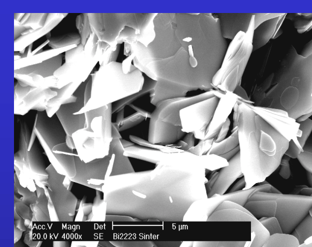

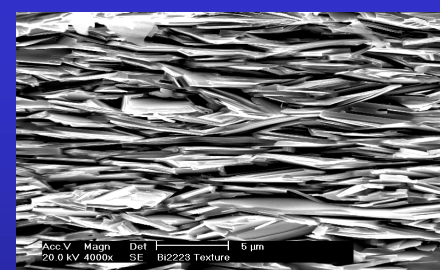

Grain alignment ⇒ ↗**Jc**

(00ℓ) Texture

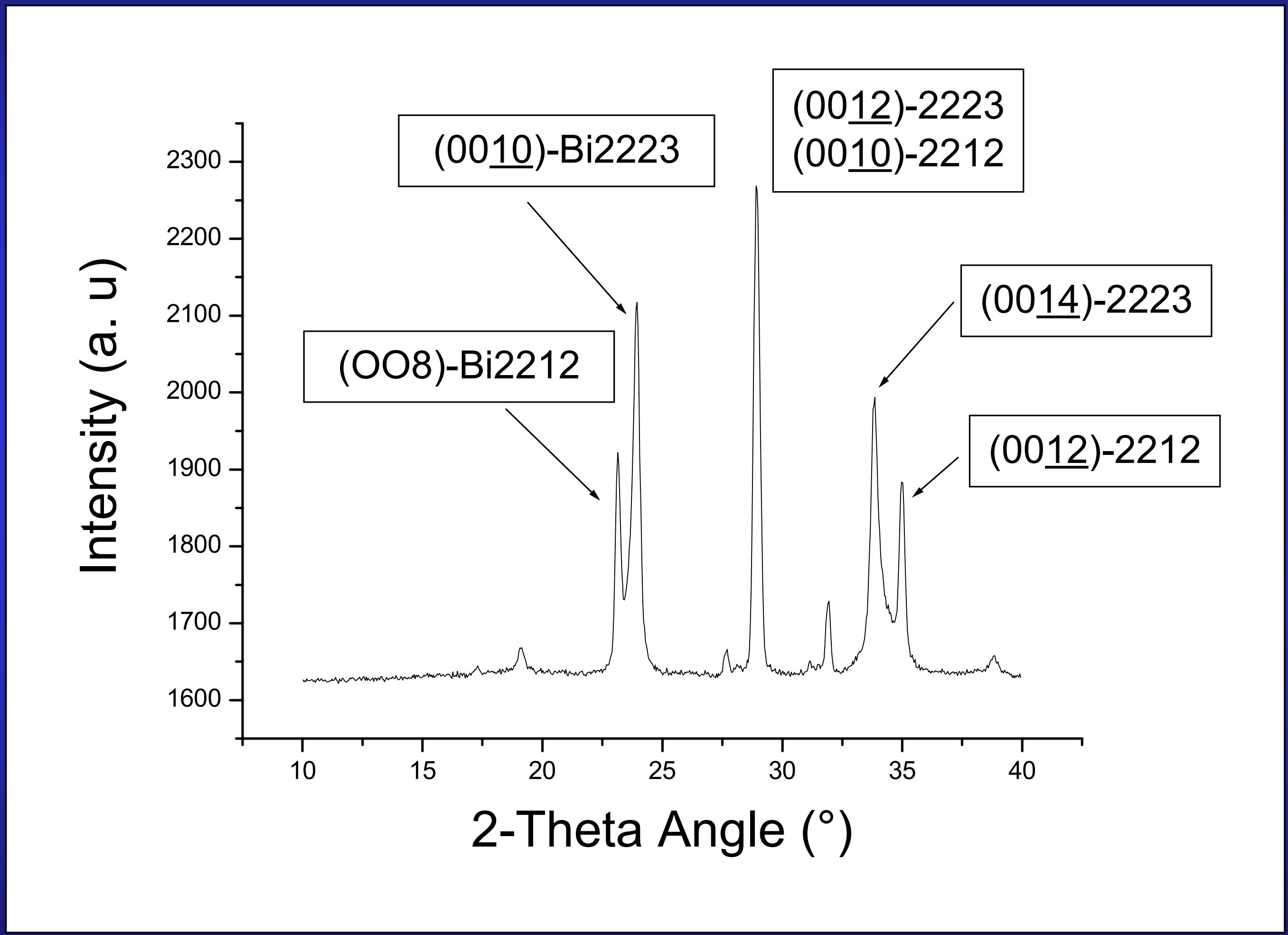

(0010)-Bi2223
(0012)-2223
(0010)-2212
(0014)-2223
(OO8)-Bi2212
(0012)-2212
Intensity (a. u)
2300
2200
2100
2000
1900
1800
1700
1600
10
15
20
25
30
35
40
2-Theta Angle (°)

Bi2212 **+** Secondary phases → **Bi2223**

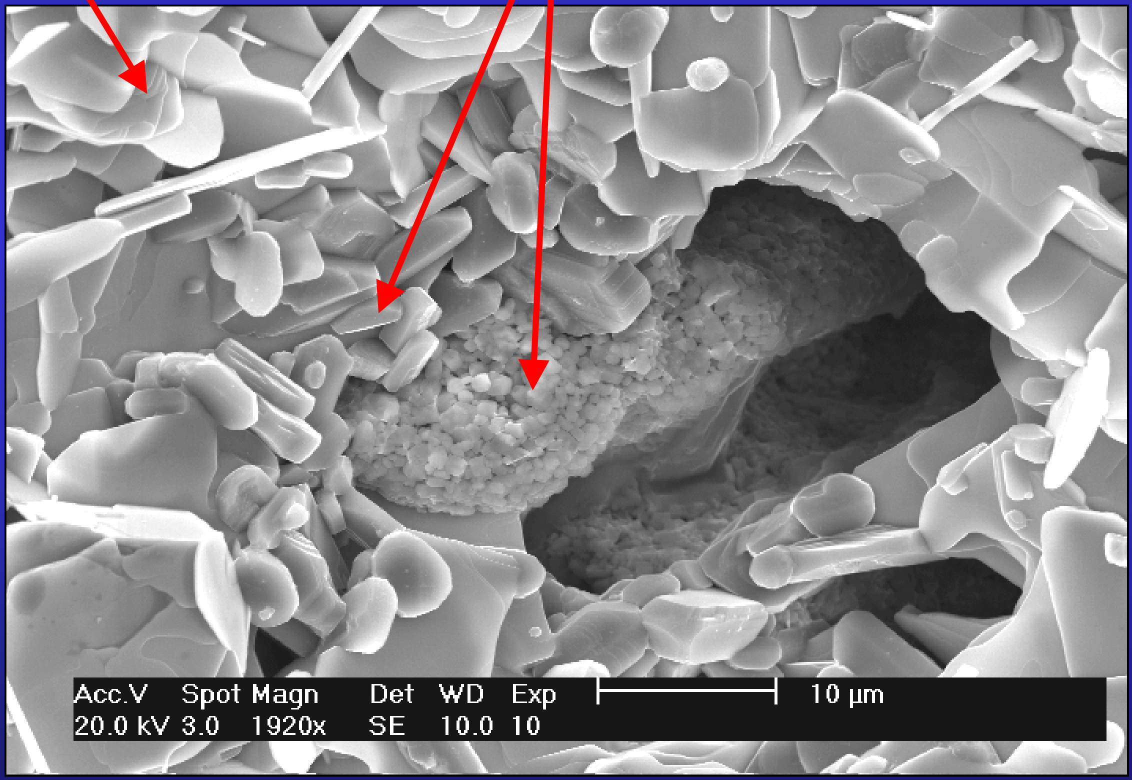

Combined Analysis

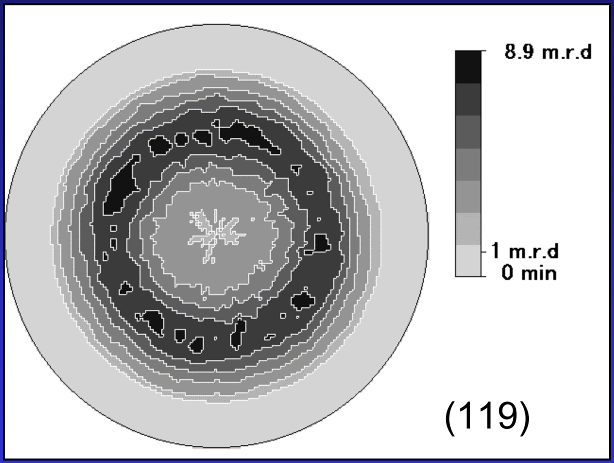

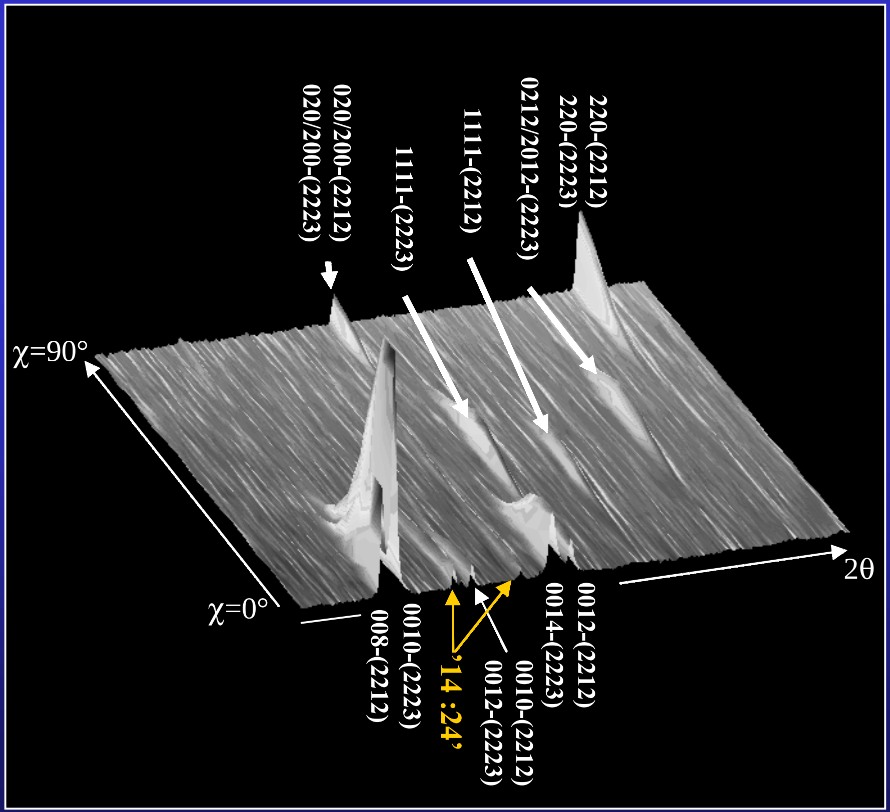

- *Neutrons*
- Sample: ~70 mm^3
- 2θ patterns for χ=0° to 90°
- No φ rotation (fibre texture).

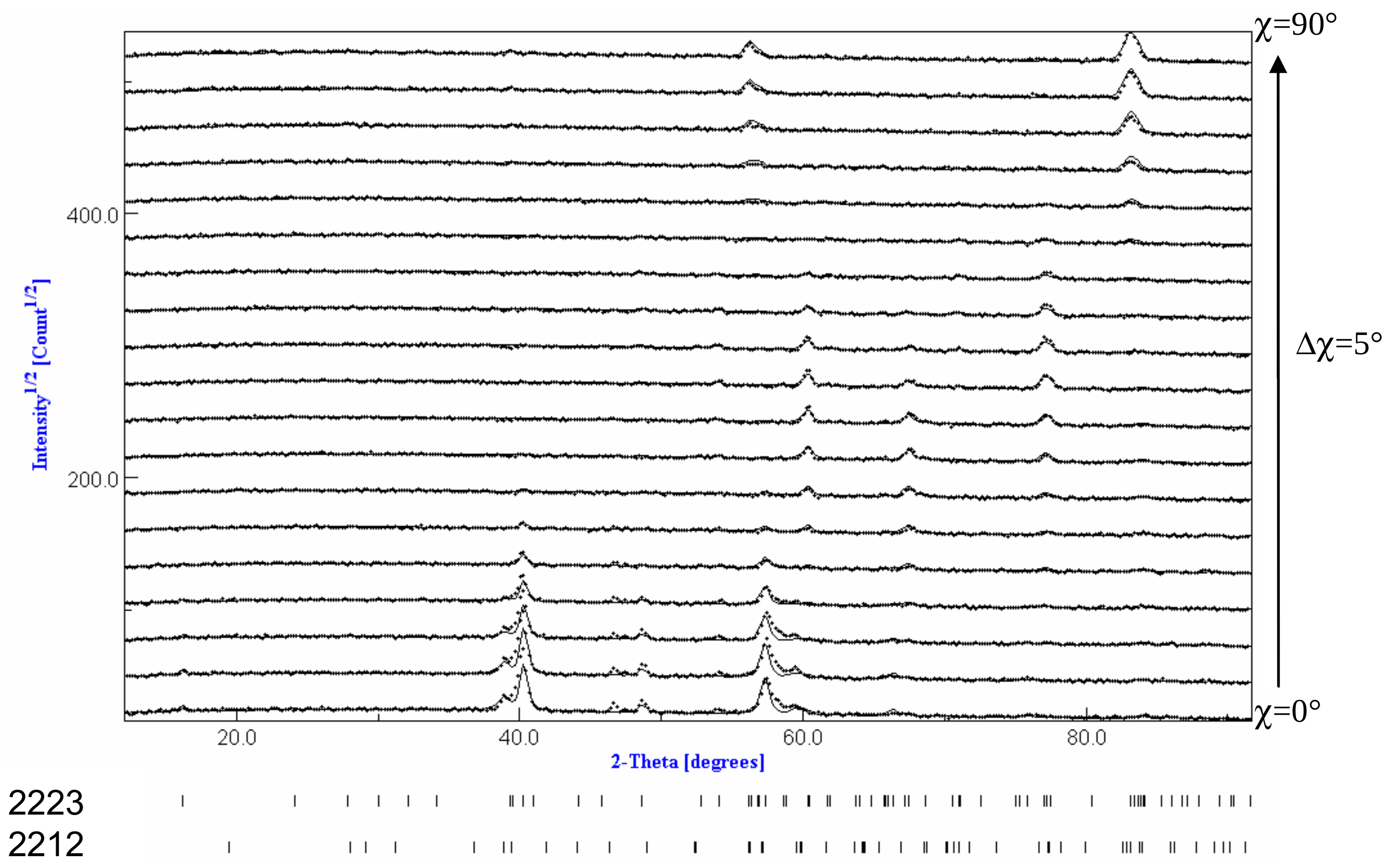

Rw=9.12
RP=16.24

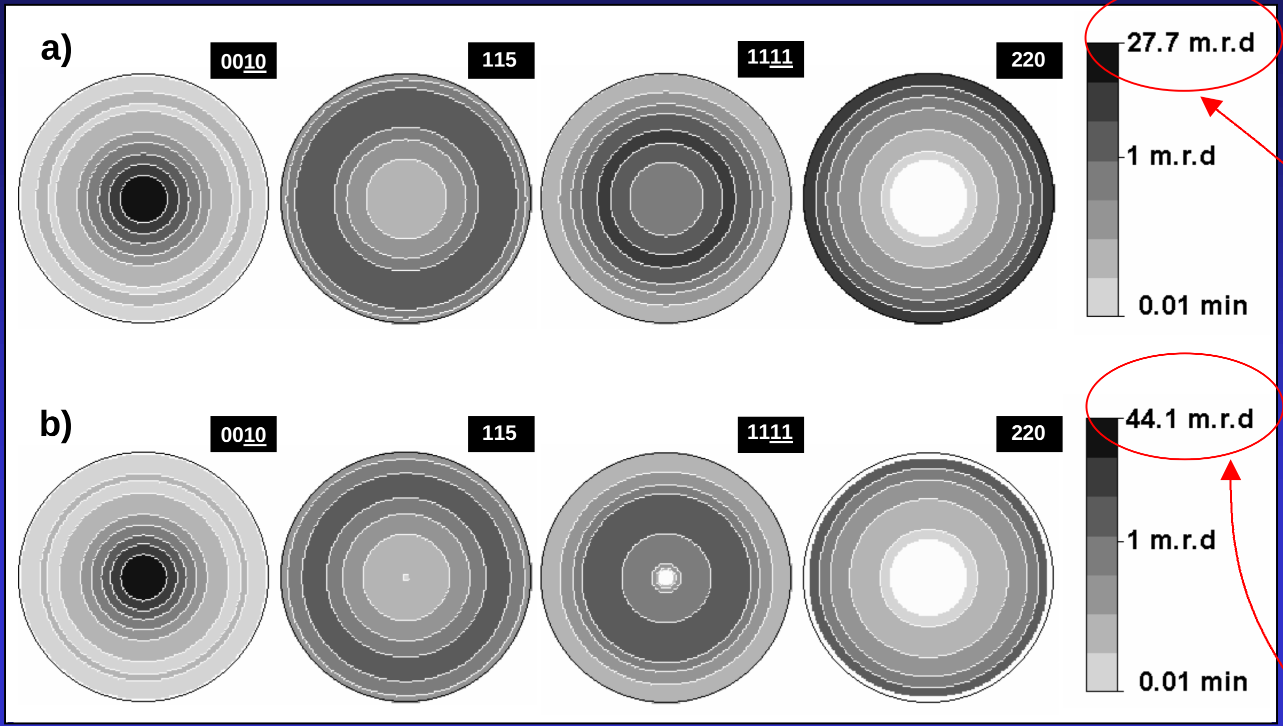

Logarithmic density scale, equal area projection

Recalculated (WIMV)

Extracted (Le Bail)

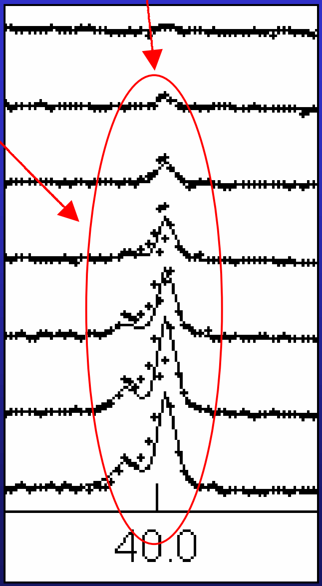

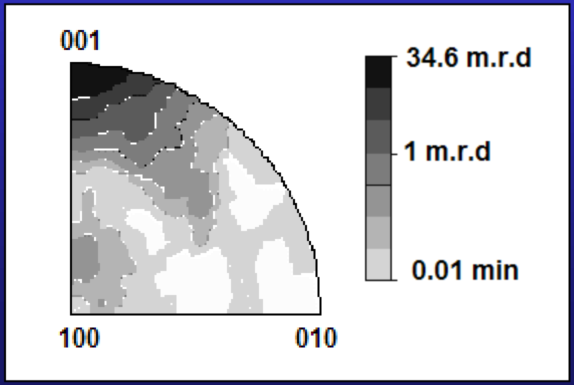

Logarithmic density scale, equal area projection

Stacking faults and/or intergrowth on the c-axis →New periodicities and peaks characterized with intermediate c parameters.

However, no algorithm is included to solve intergrowths in the combined approach.

Effect of the sinter-forging treatment on the texture development, crystal growth, transport properties

Sinter-forging dwell time (h)	*Orientation Distribution Max (m.r.d.)*		*% Bi2223*	*Cell parameters (Å)*		*Crystallite size Bi2223 (nm)*	*Rb (%)*	*Rw (%)*	*Rexp (%)*	*RP0 (%)*	*RP1 (%)*	*J_c (A/cm²)*
	Bi2212	*Bi2223*		*Bi2223*	*Bi2212*							
20	21.8	20.7	59.9±1.3	a=5.419(3) b=5.391(3) c=37.168(3)	a=5.414(3) b=5.393(3) c=30.800(3)	205±7	7.56	11.1	4.55	17.74	10.56	12500
50	24.1	24.4	72.9±2.9	a=5.419(3) b=5.408(3) c=37.192(3)	a=5.416(3) b=5.396(3) c=30.806(3)	273±10	7.54	11.37	4.58	17.05	11.04	15000
100	31.5	25.2	84.4±4.6	a=5.410(3) b=5.405(3) c=37.144(3)	a=5.412(3) b=5.403(3) c=30.752(3)	303±10	5.4	8.04	3.69	13.54	9.31	19000
150	65.4	27.2	87.0±4.1	a=5.417(3) b=5.403(3) c=37.199(3)	a=5.413(3) b=5.407(3) c=30.792(3)	383±13	6.13	9.12	4.8	16.24	12.25	20000

Texture strength

Sinter-forging Time

% Bi2223

J_c

Crystallite Size

E. Guilmeau et al., JAC

$Ca_3Co_4O_9$ *thermoelectrics*

J.G. Noudem, Caen

$Ca_3Co_4O_9$: Misfit lamellar and modulated Structure, with high thermopower

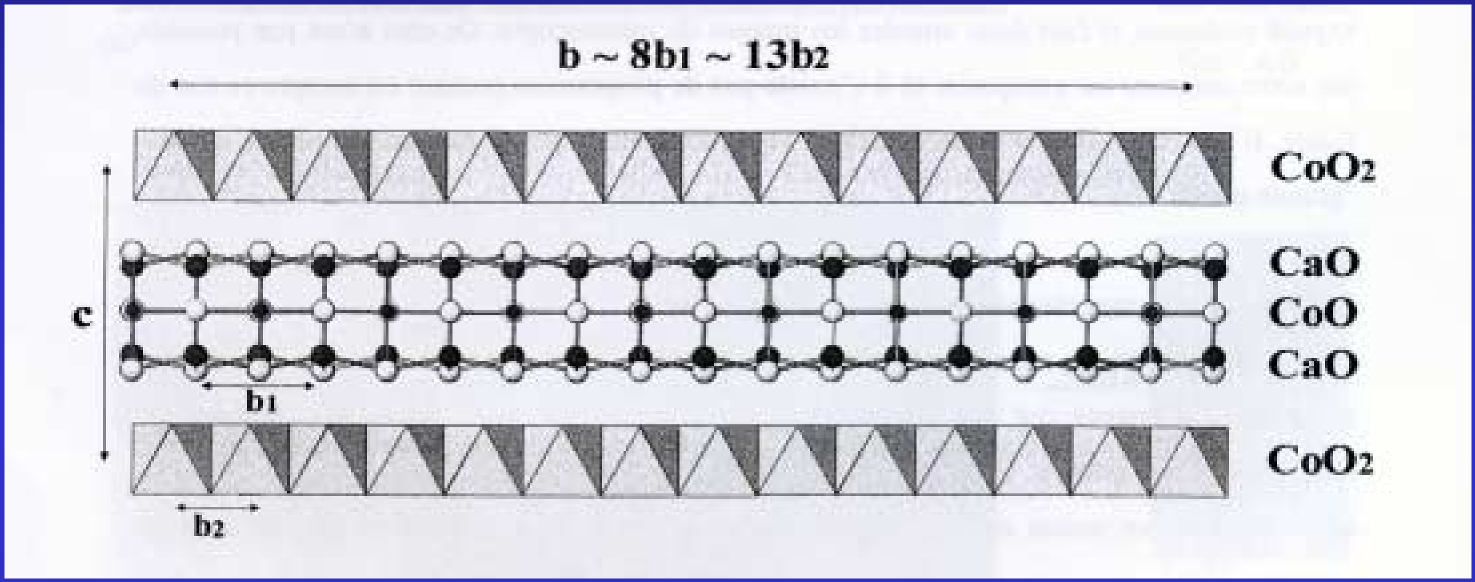

Two monoclinic sub-systems:

S1 with a ~ 4.8Å, b_1 ~ 4.5Å, c ~ 10.8Å et β ~ 98° (NaCl-type)

S2 with a ~ 4.8Å, b_2 ~ 2.8Å, c ~ 10.8Å et β ~ 98° (CdI_2-type)

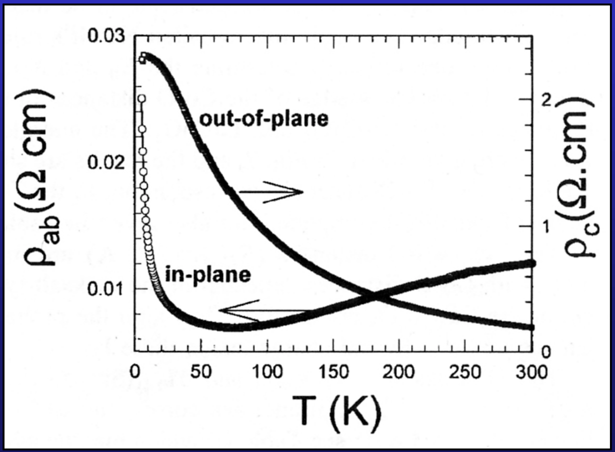

$\Gamma=\sigma_{ab}/\sigma_c \sim 10$ → Texture

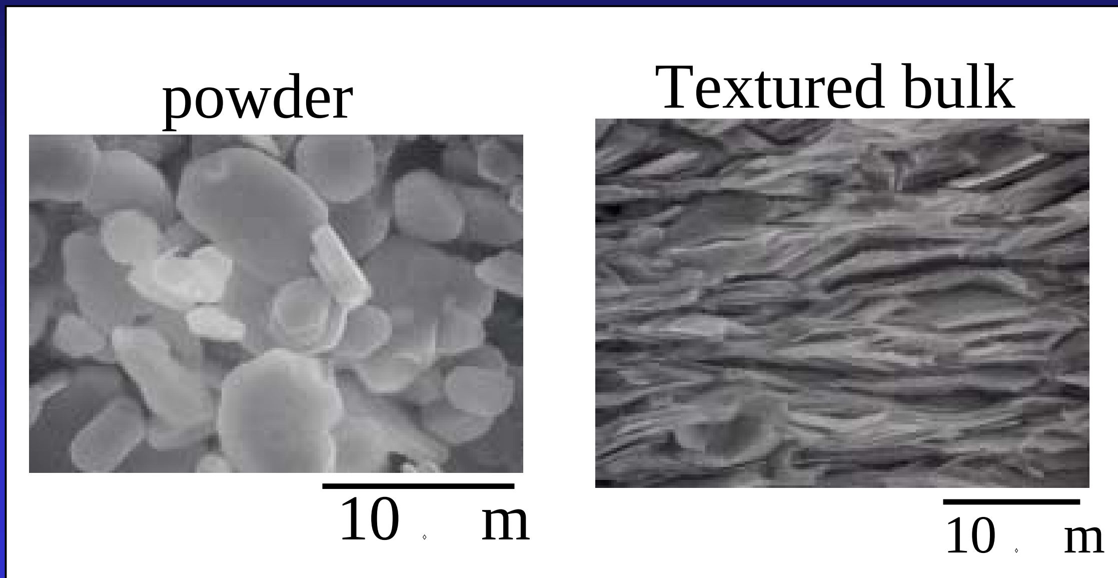

Magnetic alignment
and
Templated Growth
method

Analysis:

- *neutrons*
- *3D Supercell: a=4.8309Å, b~8b1~13b2~36.4902Å, c=10.8353Å, β=98.13°*
174 atoms/cell
-*Sample : 0.6 cm^3*

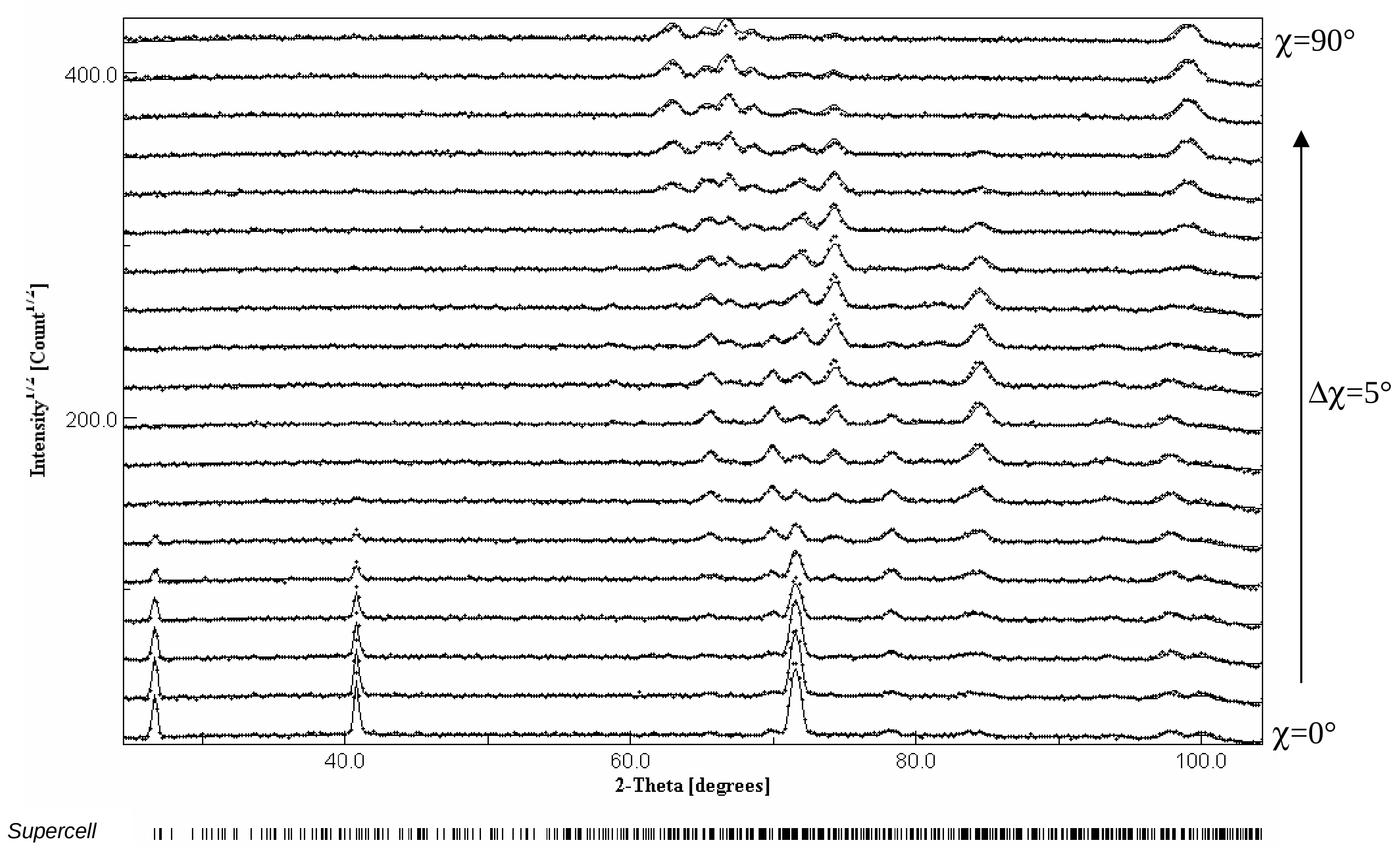

χ=90°
Δχ=5°
χ=0°
400.0
200.0
Intensity^1/2 [Count^1/2]
40.0
60.0
80.0
100.0
2-Theta [degrees]
Supercell

RP=19.7%, Rw=11.9%

9.8 MPa for 2 h

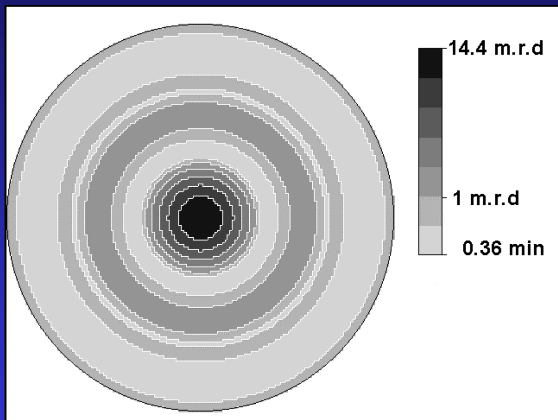

19.6 MPa for 6 h

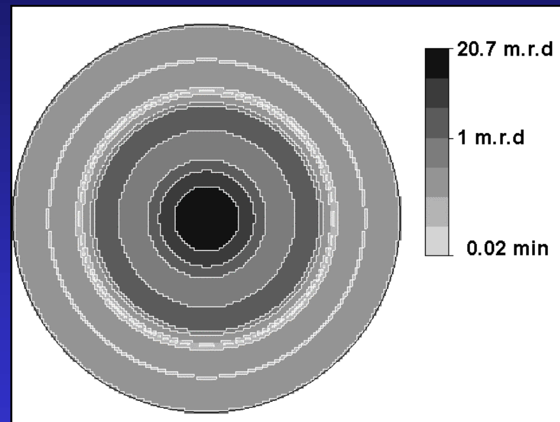

19.6 MPa for 20 h

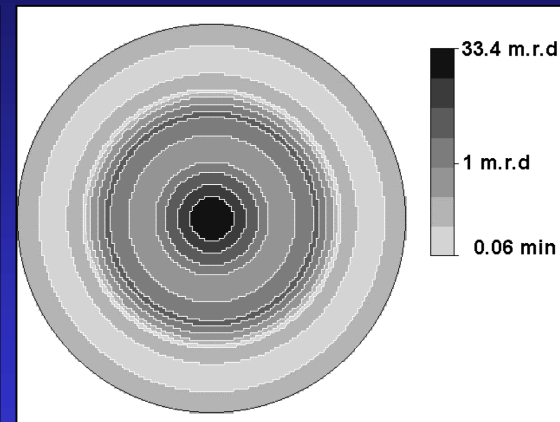

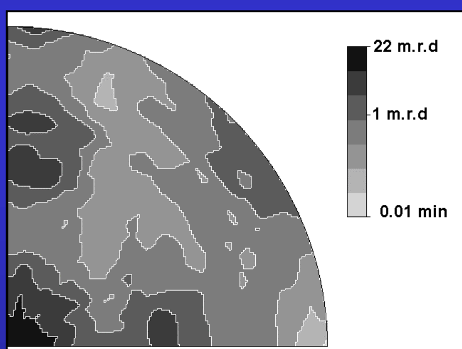

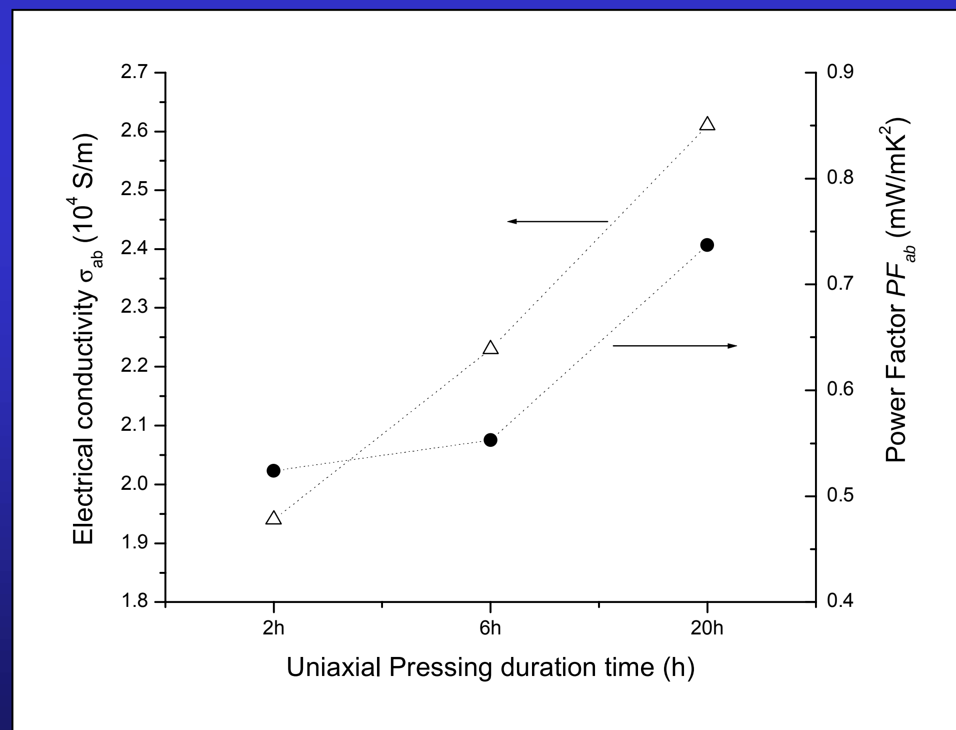

Templated Growth Method

Magnetic Alignment

Logarithmic density scale, equal area projection

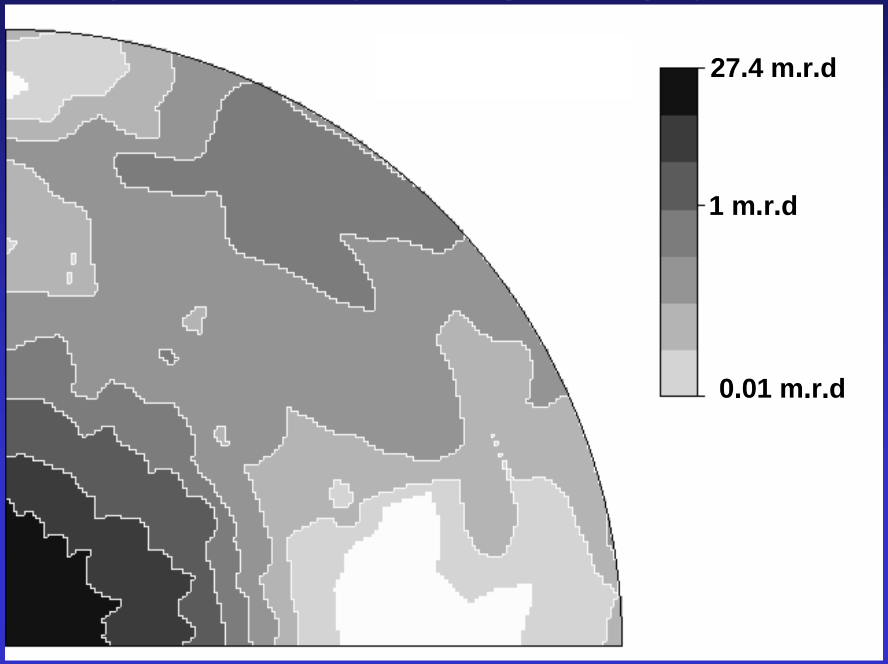

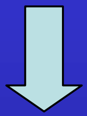

- magnetic alignment really efficient to obtain strong textures

- combined analysis of modulated structures possible

Ferroelectric PCT films

J. Ricote, Madrid

thin films:

$(Ca_{0.24}Pb_{0.76})TiO_3$ sol-gel synthesised solutions deposited by spin coating on a substrate of $Pt/TiO_2/Si$, with and without a treatment at 650ºC for 30 min.

All films are crystallised at 700ºC for 50 s by Rapid Thermal Processing (RTP; 30ºC/s). A series is also recrystallised at 650ºC for 1 to 3 h.

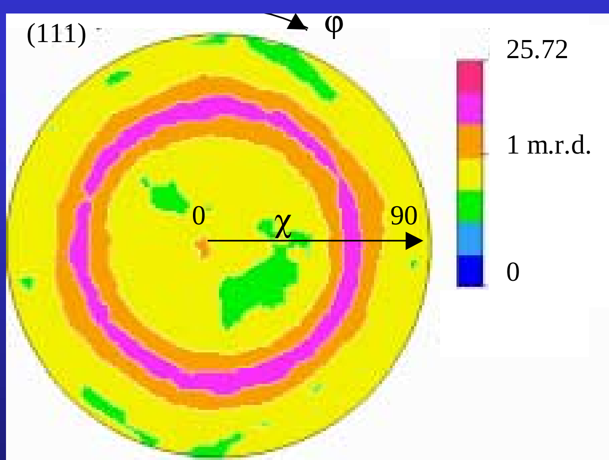

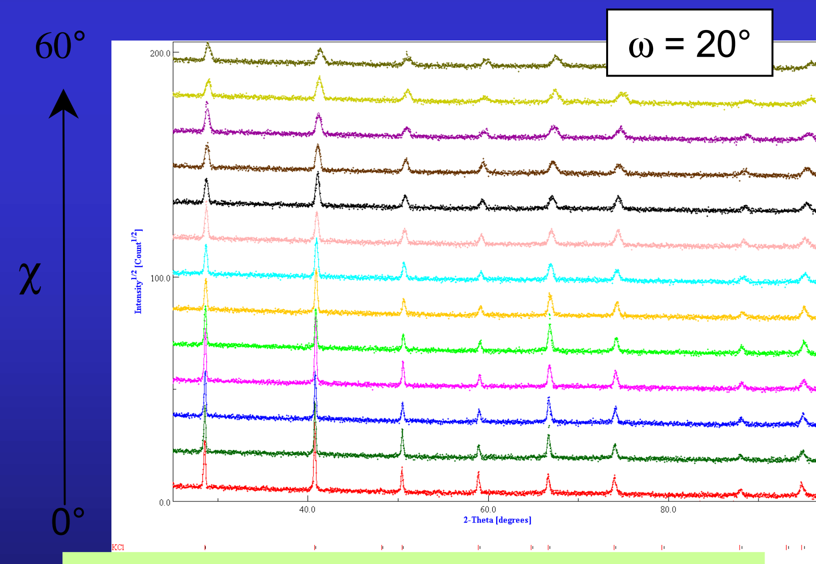

Refinement of individual spectra

Limitations of the simple Quantitative Texture Analysis

Structural parameters are difficult to obtain due to:

Substrate influence:
overlapping of reflections from the film and the substrate

TEXTURE effects:
peaks that do not appear at low χ angles

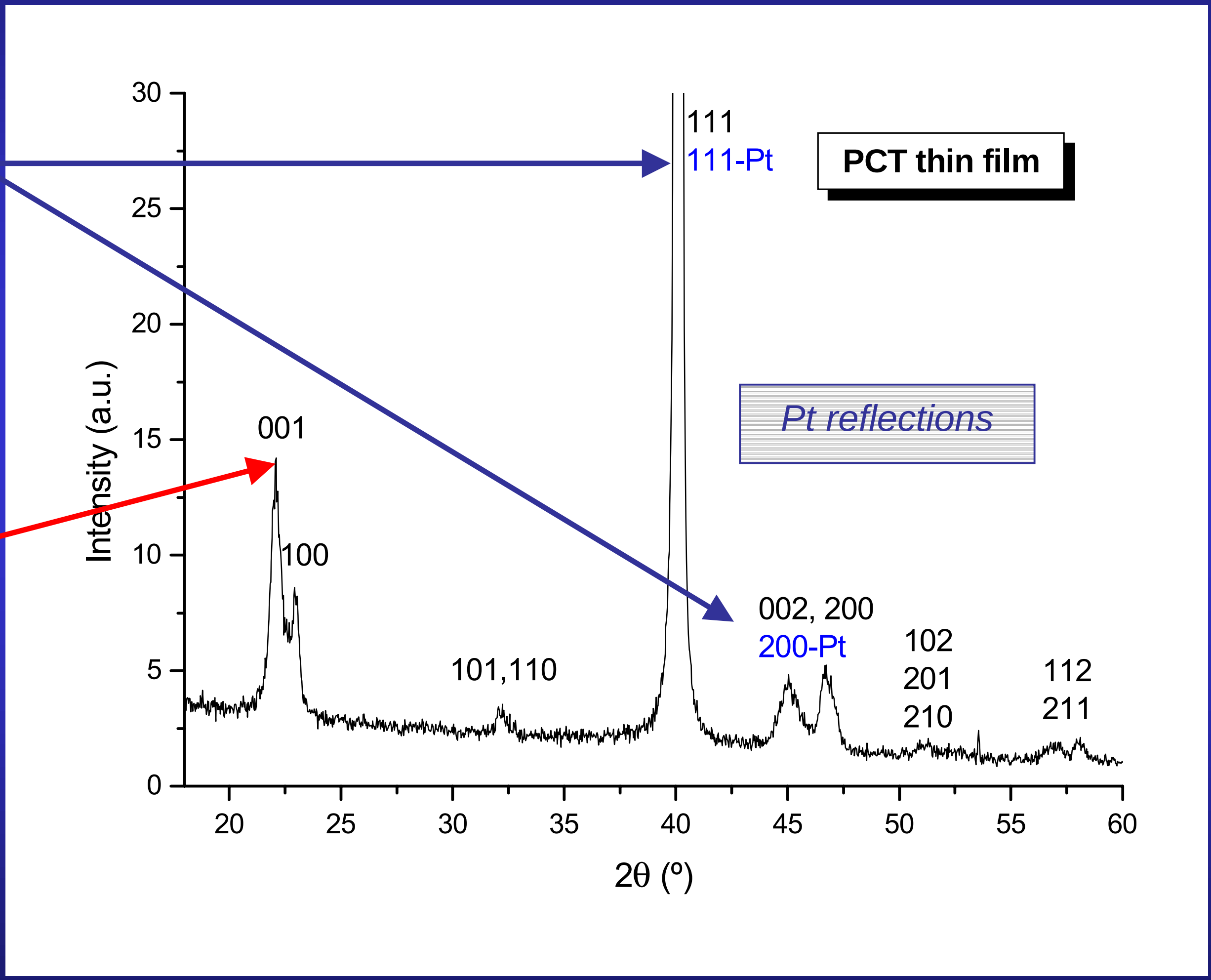

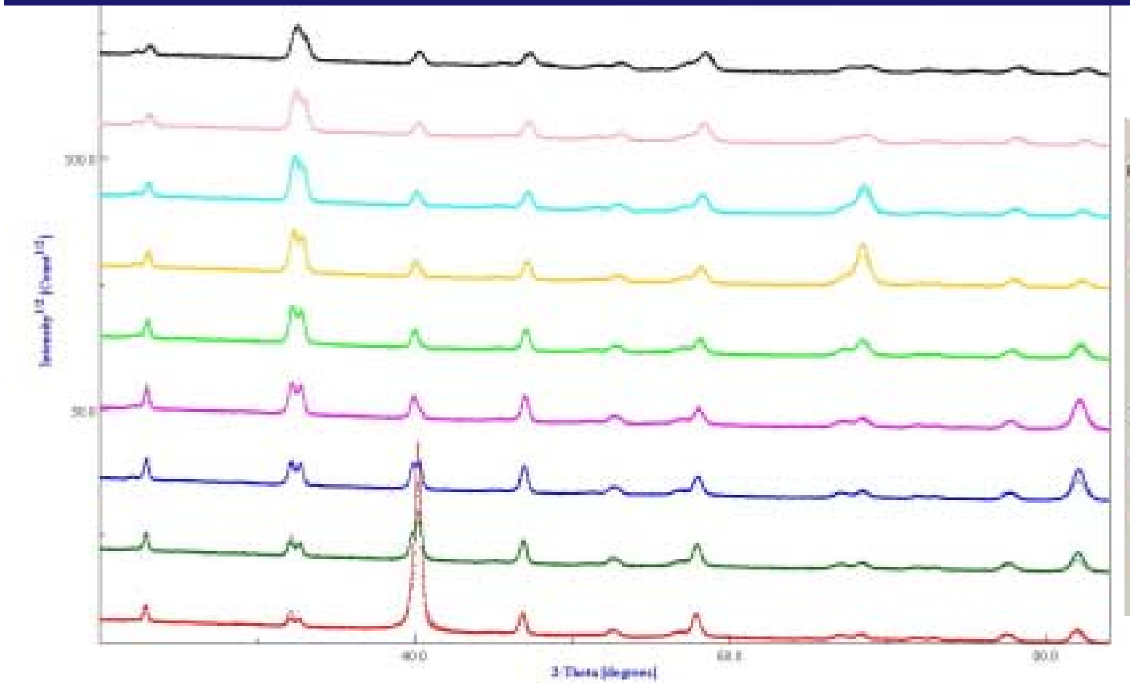

PCT

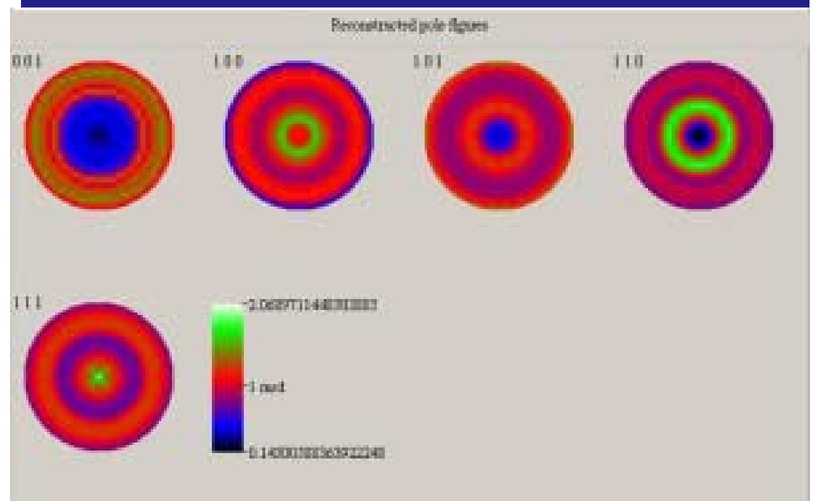

a = 3.9156(1) Å

c = 4.0497(3) Å

T = 2525(13) Å

t_{iso} = 390(7) Å

ε = 0.0067(1) rms

Pt

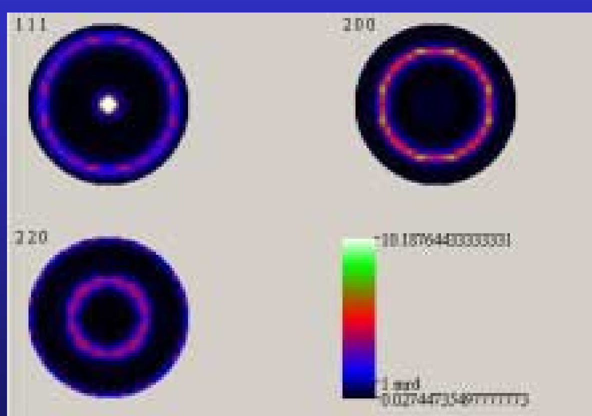

a = 3.9108(1) Å

T = 457(3) Å

t_{iso} = 458(3) Å

ε' = 0.0032(1) rms

R_W = 13%; R_B = 12%; R_{exp} = 22%.(Rietveld)

R_W = 5%; R_B = 6% (E-WIMV)

Atom	Occupancy	x	y	z
Pb	0.76	0.0	0.0	0.0
Ca	0.24	0.0	0.0	0.0
Ti	1.0	0.5	0.5	0.477(2)
O1	1.0	0.5	0.5	0.060(2)
O2	1.0	0.0	0.5	0.631(1)

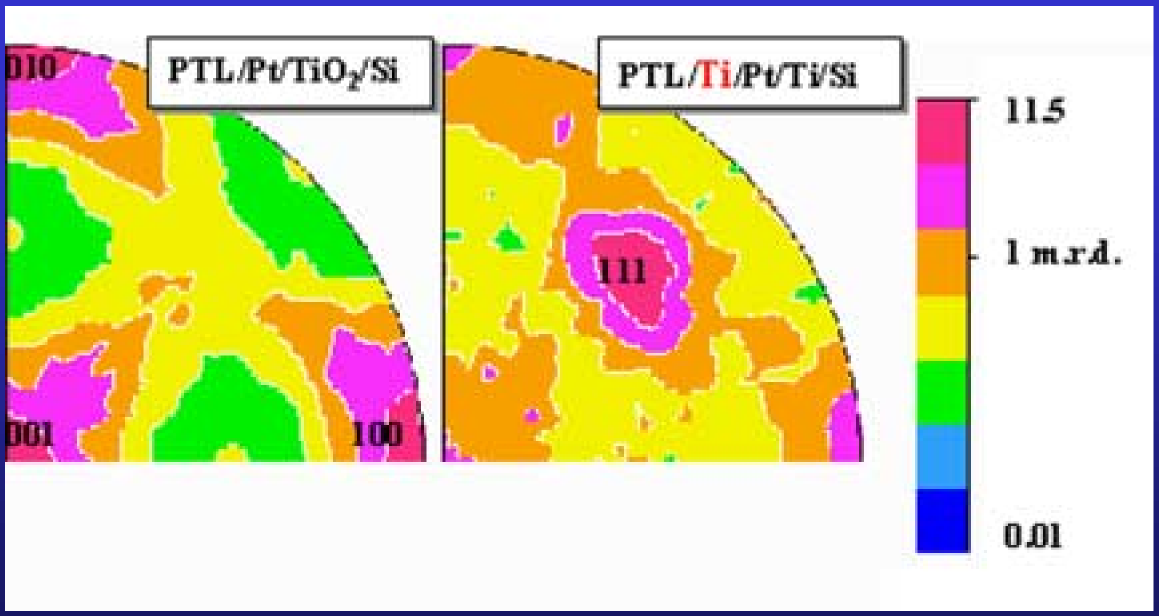

Structural parameters

Pt layer

	a (Å)	thickness (nm)	R factors (%)
non-treated substrate			
Pt	3.9108(1)	45.7(3)	R_W=13, R_B=12, R_{exp}=22
annealed substrate			
Pt	3.9100(4)	46.4(3)	R_W=8, R_B=14, R_{exp}=21
Pt (Recryst. 1h)	3.9114(2)	47.8(3)	R_W=9, R_B=20, R_{exp}=21
Pt (Recryst. 2h)	3.9068(1)	46.9(3)	R_W=9, R_B=14, R_{exp}=22
Pt (Recryst. 3h)	3.9141(4)	47.5(9)	R_W=27, R_B=12, R_{exp}=21

Annealing of the substrate does not introduce significant variations on the structure of the Pt layer

PTC film

	a (Å)	c (Å)	thickness (nm)
on non-treated substrate			
PCT	3.9156(1)	4.0497(6)	272.5(13)
on annealed substrate			
PCT	3.8920(6)	4.0187(8)	279.0(9)
PCT (Recryst. 1h)	3.8929(2)	4.0230(4)	266.1(11)
PCT (Recryst. 2h)	3.8982(2)	4.0227(4)	258.4(9)
PCT (Recryst. 3h)	3.9001(4)	4.0228(11)	253.6(29)

Recrystallisation reduces the stress on the film, and, increases the lattice parameters

Structural, microstructural and texture quantitative characterisation of ferroelectric thin films by the combined method

Analysis of the X-ray diffraction diagrams of a PCT film on $Pt/TiO_2/Si$

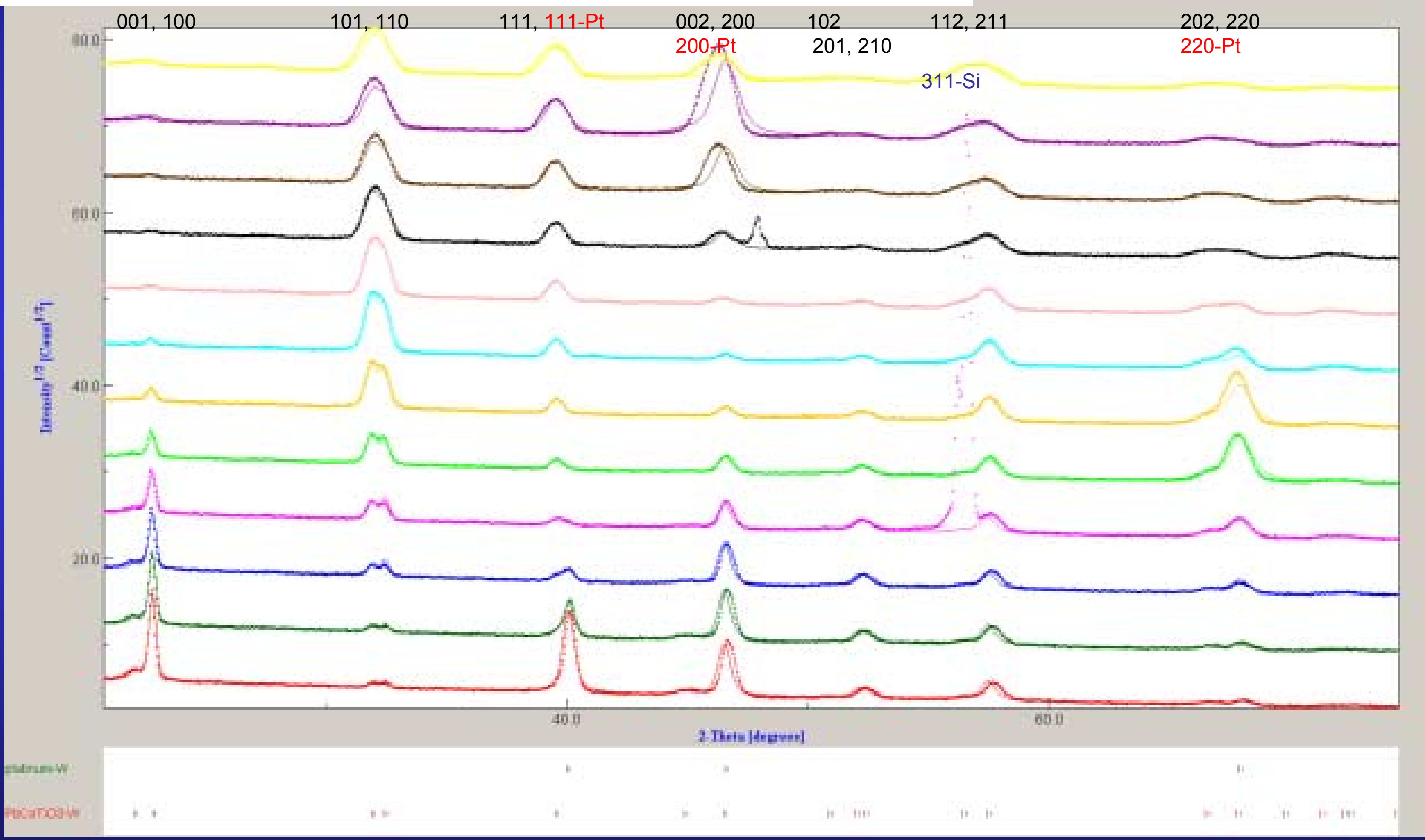

R_W = 13%; R_B = 12%; R_{exp} = 22%.(Rietveld)
R_W = 5%; R_B = 6% (E-WIMV)

Substrate influence on Residual Stress and Texture

Tensile stress

PCT on $Pt/TiO_2/(100)Si$

PCT on $Pt/(100)MgO$

PCT on $Pt/(100)SrTiO_3$

Compressive stress

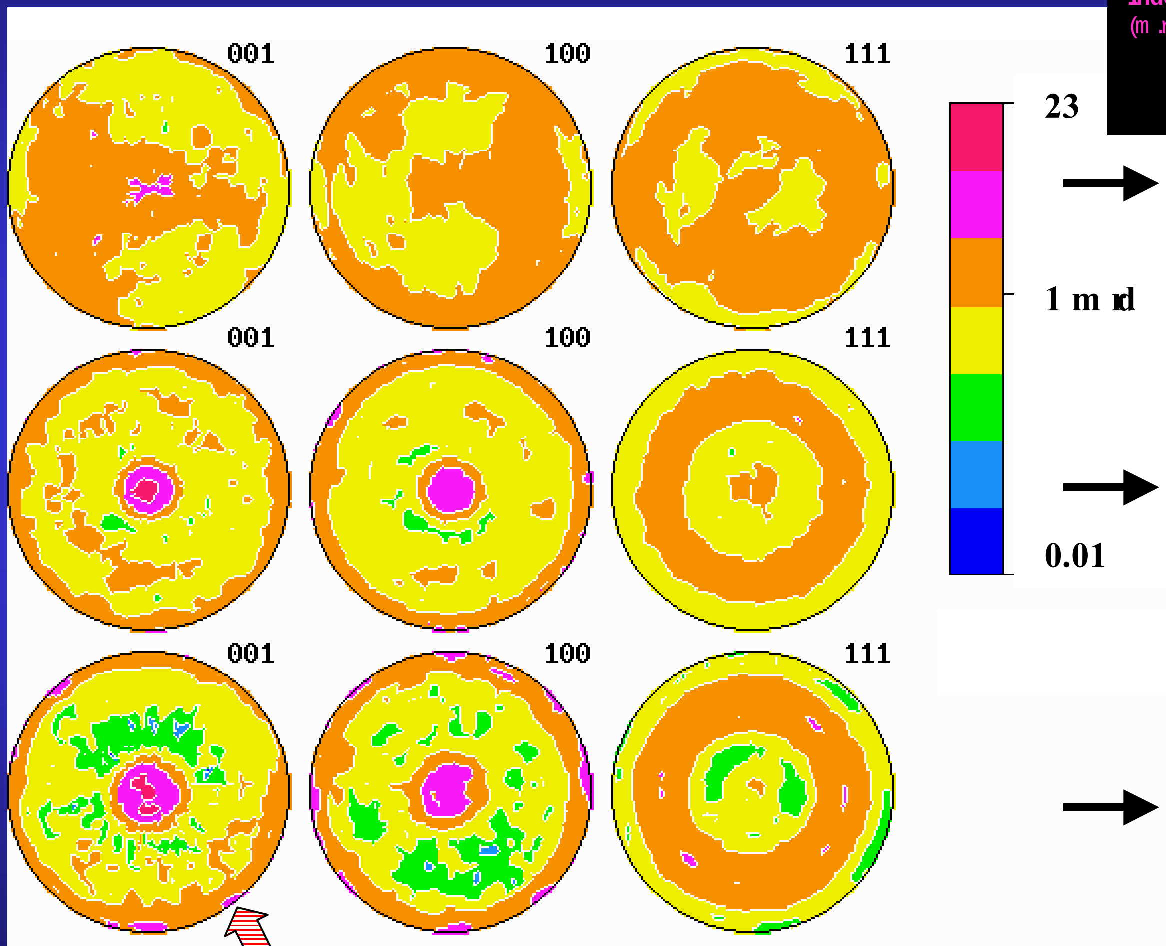

Enhancement of <001> texture

	Texture Index (m.r.d.^{2})	Pyroelectric Coefficient (10^{-8}C cm^{-2} K^{-1})
PCT on $Pt/TiO_2/(100)Si$	2.1	0.3
PCT on $Pt/(100)MgO$	5.1	1.5
PCT on $Pt/(100)SrTiO_3$	7.9	1.1

Compliance coefficients [10^{-3} GPa^{-1}]	$PbTiO_3$ single crystal (data set A)	Film random orientation	PCT-Si <001> contrib≈17%	PLT <001> contrib.≈49%	PCT-Mg <001> contrib.≈68%
s_{11}	6.5	10.1	10.5	10.0	9.7
s_{22}	6.5	10.0	10.5	10.0	9.7
s_{33}	33.3	9.8	9.0	10.3	11.3
s_{44}	14.5	13.2	12.8	12.9	13.1
s_{55}	14.5	13.2	12.8	13.0	13.1
s_{66}	9.6	13.4	14.0	13.5	12.7
s_{12}	-0.35	-3.3	-3.5	-3.2	-3.0
s_{21}	-0.35	-3.3	-3.5	-3.2	-3.0
s_{13}	-7.1	-3.2	-3.1	-3.4	-3.6
s_{31}	-7.1	-3.2	-3.1	-3.4	-3.6
s_{23}	-7.1	-3.2	-3.1	-3.4	-3.6
s_{32}	-7.1	-3.2	-3.1	-3.4	-3.6
s_{33}/s_{11}	5.1	0.97	0.86	1.03	1.16
s_{13}/s_{12}	20.3	0.97	0.89	1.06	1.20

Geometric mean average + biaxial stress state

Si nanocrystalline thin films

M. Morales, Caen

Silicon thin films deposition by reactive magnetron sputtering:

- power density 2W/cm^2
- total pressure: p_{total} = 10^{-1} Torr
- plasma mixture: H_2 / Ar, pH_2 / p_{total} = 80 %
- temperature: 200°C
- substrates: amorphous SiO_2 (a-SiO_2)
  (100)-Si single-crystals
- target-substrate distance (d)
  - a-SiO_2 substrates: d = 4, 6, 7, 8, 10, 12 cm
    films A, B, C, D, E, F
  - (100)-Si: d = 6, 12 cm
    films G, H

Aim: quantum confinement, photoluminescence properties

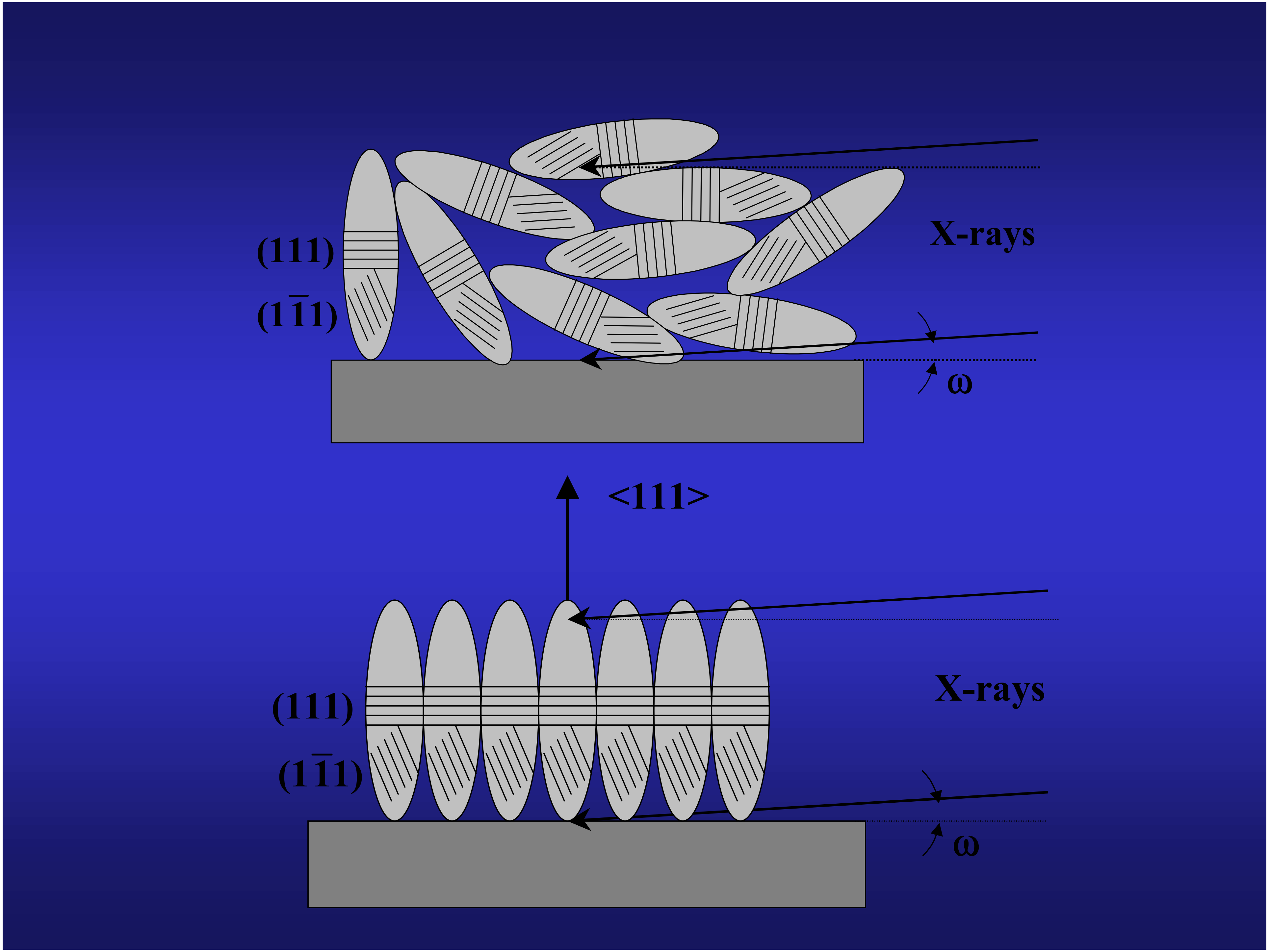

X-rays
(111)
$(1\bar{1}1)$
ω
<111>
X-rays
(111)
$(1\bar{1}1)$
ω

Typical refinement

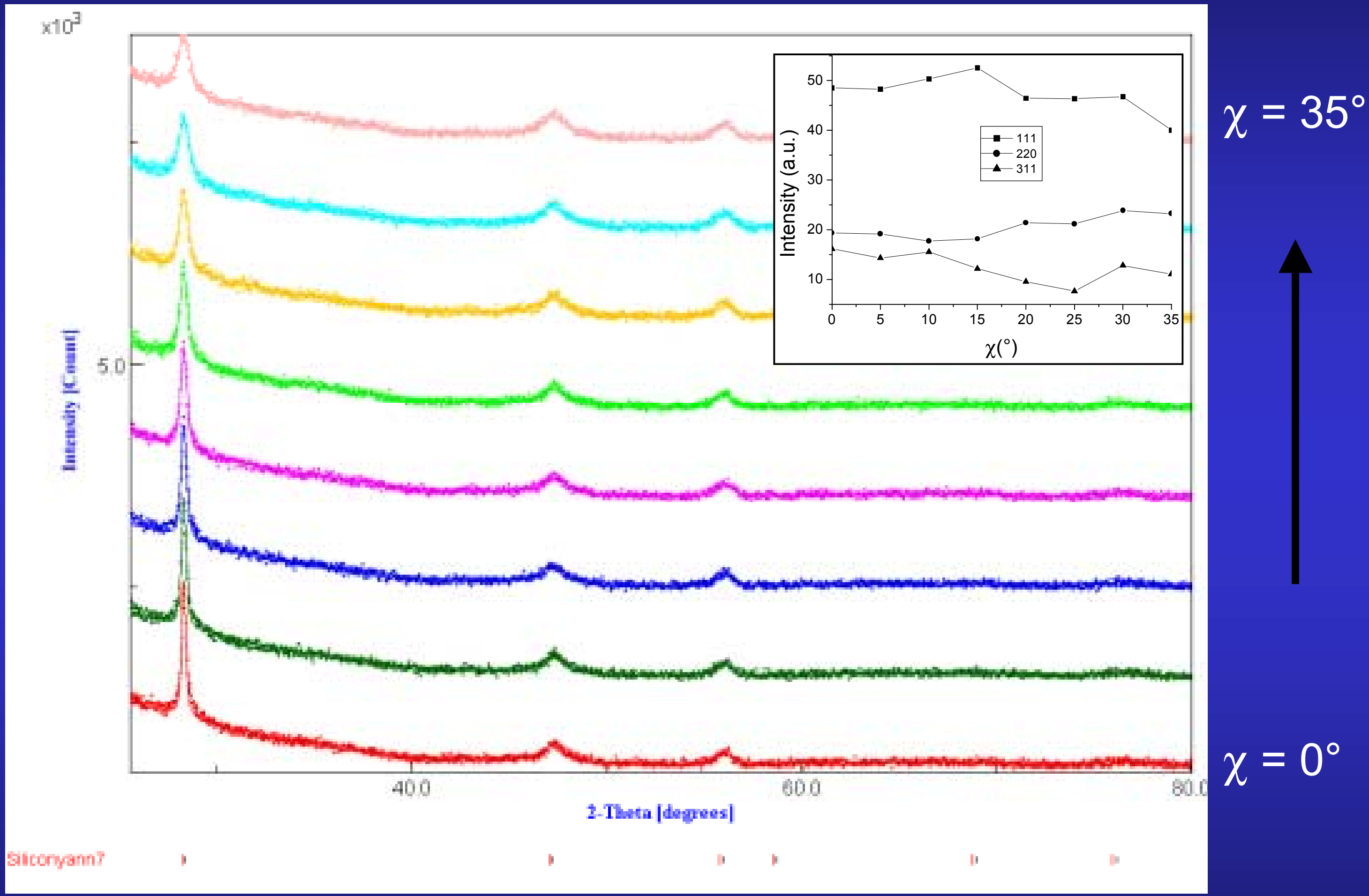

broad, anisotropic diffracted lines, textured samples

Refinement Results

Sample	d (cm)	a (Å)	RX thickness (nm)	Anisotropic sizes (Å)			Texture parameters			Reliability factors (%)			
				<111>	<220>	<311>	Maximum (m.r.d.)	minimum (m.r.d.)	Texture index F^2 (m.r.d^2)	RP_0	R_w	R_B	R_{exp}
A	4	5.4466 (3)	---	94	20	27	1.95	0.4	1.12	1.72	4.0	3.7	3.5
B	6	5.4439 (2)	711 (50)	101	20	22	1.39	0.79	1.01	0.71	4.9	4.3	4.2
C	7	5.4346 (4)	519 (60)	99	40	52	1.72	0.66	1.05	0.78	4.3	4.0	3.9
D	8	5.4461 (2)	1447 (66)	100	22	33	1.57	0.63	1.04	0.90	5.5	4.6	4.5
E	10	5.4462 (2)	1360 (80)	98	20	25	1.22	0.82	1.01	0.56	5.0	3.9	4.0
F	12	5.4452 (3)	1110 (57)	85	22	26	1.59	0.45	1.05	1.08	4.2	3.5	3.7
G	6	5.4387 (3)	1307 (50)	89	22	28	1.84	0.71	1.01	1.57	5.2	4.7	4.2
H	12	5.4434 (2)	1214 (18)	88	22	24	2.77	0.50	1.12	2.97	5.0	4.5	4.3

Mean anisotropic shape

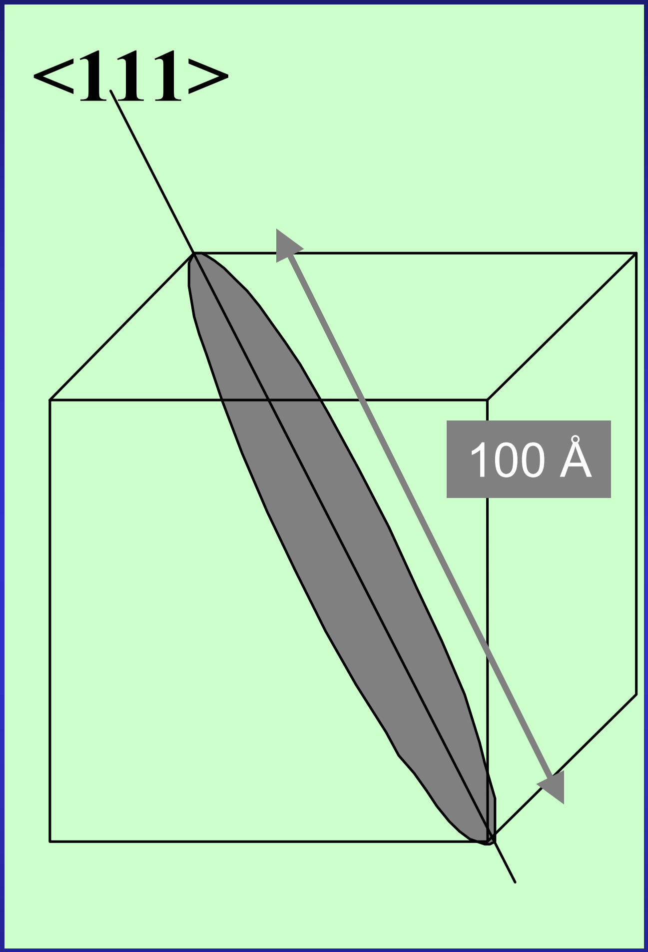

Schematic of the mean crystallite shape for Sample D represented in a cubic cell, as refined using the Popa approach and exhibiting a strong elongation along <111> (see Table).

001 Inverse Pole Figures

a-SiO_2

(100)-Si

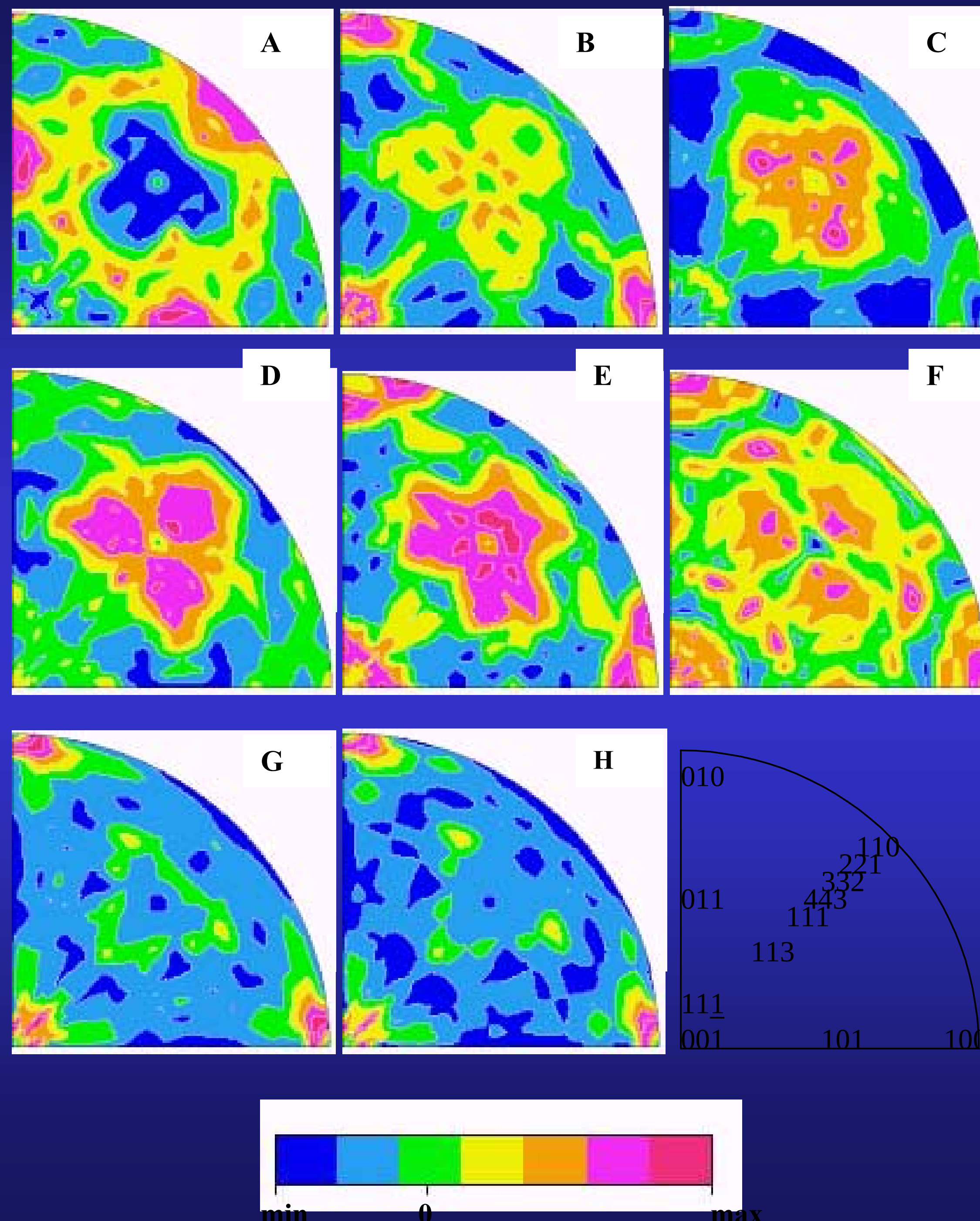

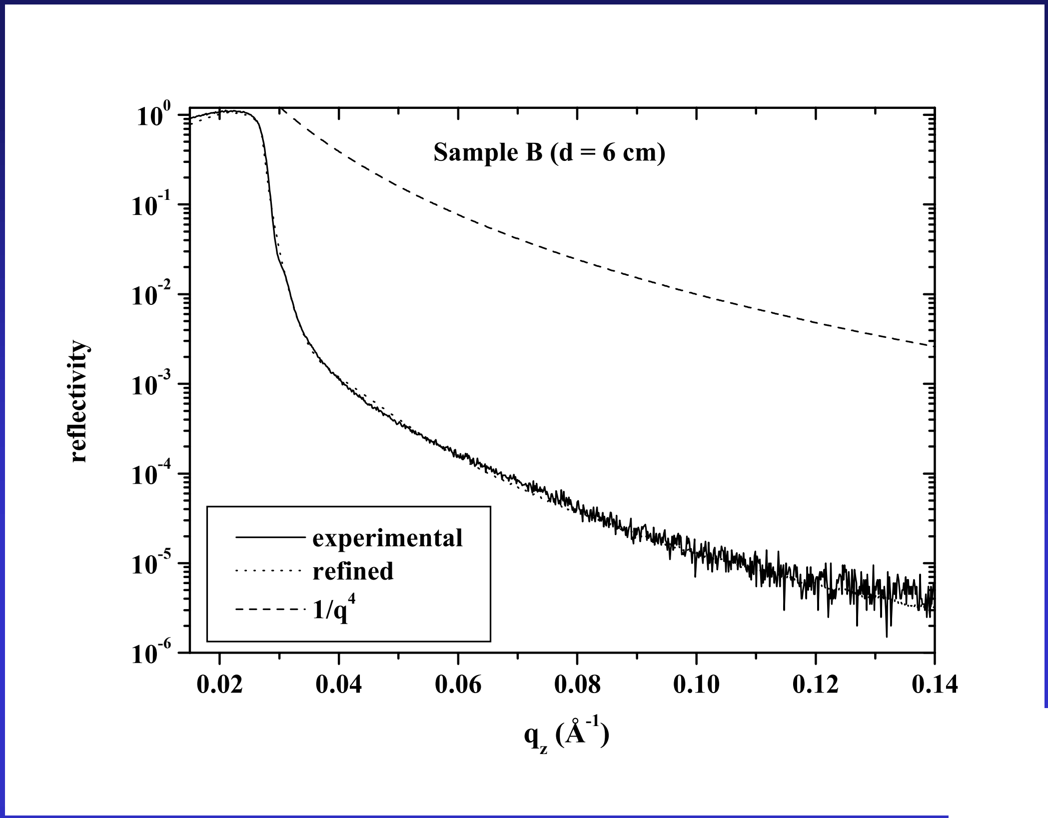

XRR:

Roughness governed

AFM:

homogeneous

roughness

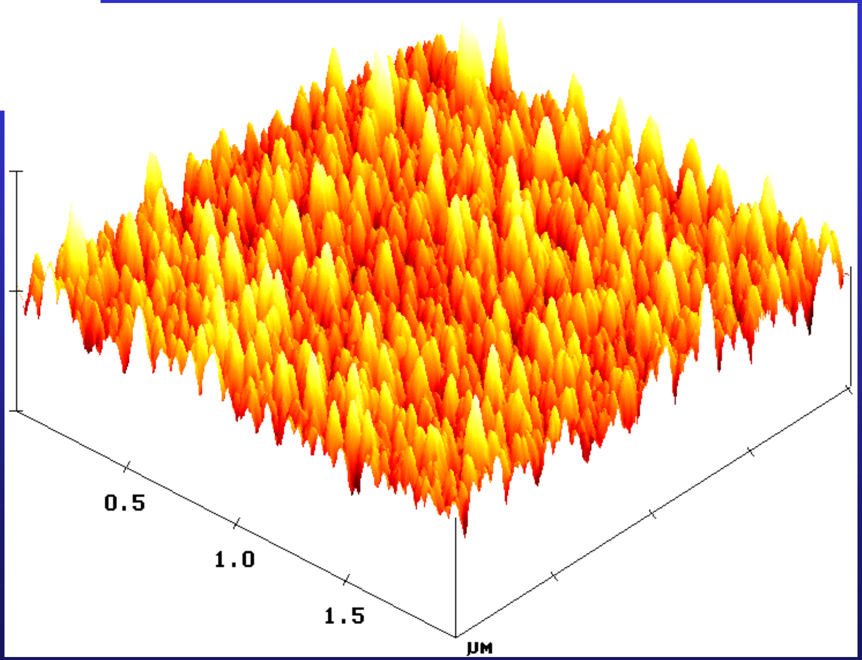

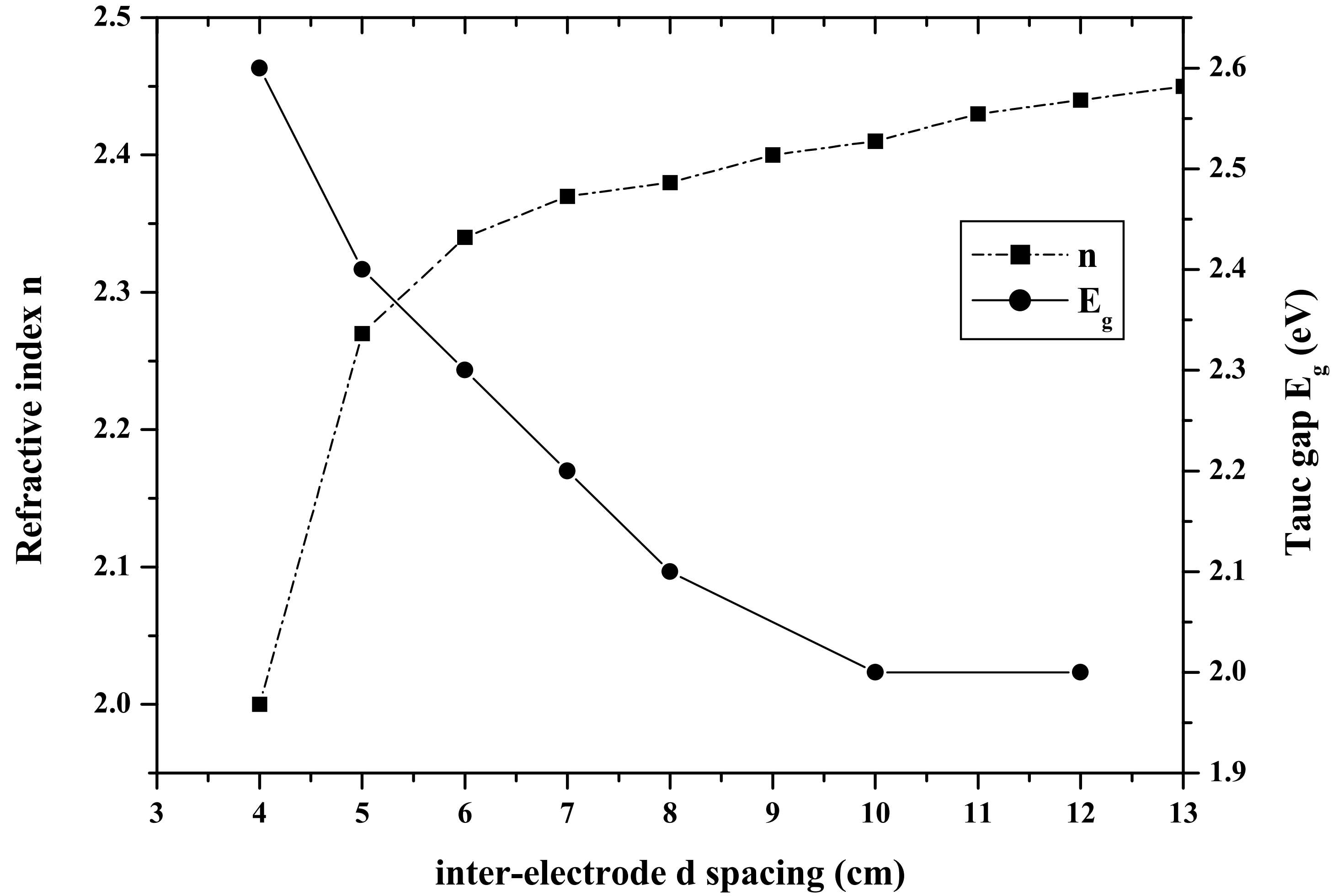

Refractive index n
Tauc gap E_g (eV)
inter-electrode d spacing (cm)
n
E_g
2.0
2.1
2.2
2.3
2.4
2.5
1.9
2.0
2.1
2.2
2.3
2.4
2.5
2.6
3
4
5
6
7
8
9
10
11
12
13

Irradiated FluorApatite (FAp) ceramics

S. Miro, PhD

Self-recrystallisation under irradiation, depending on SiO_4 / PO_4 ratio (FAp / Nd-Britholite) and on irradiating species

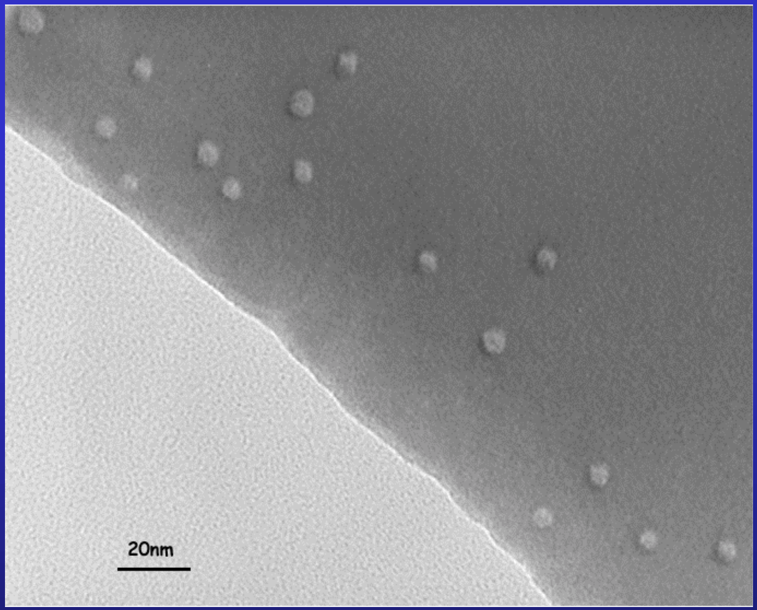

TEM of FAp irradiated with 70 MeV, 10^{12} Kr cm^{-2} ions

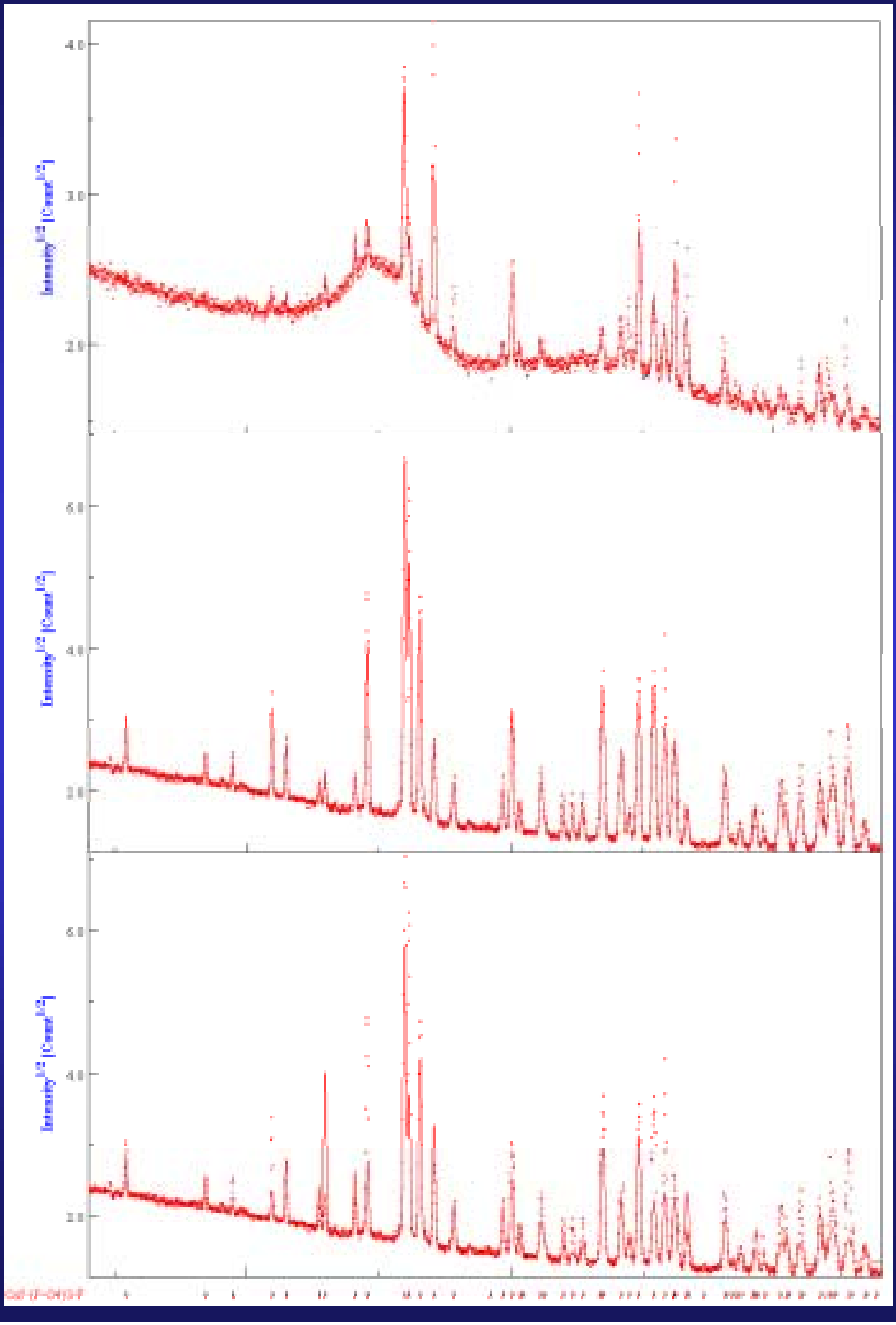

texture corrected,

10^{13} Kr cm^{-2}

Virgin, with texture correction

Virgin, no texture correction

Fluence (ions.cm^{-2})	Vc/V (%)	A (Å)	c (Å)	<t> (nm)	$\Delta a/a_0$ (%)	$\Delta c/c_0$ (%)	R_w (%)	R_B (%)
0	100	9.3365(3)	6,8560(5)	294(22)	-	-	14.6	9.1
Kr								
10^{11}	100	-	-	-	-	-		
10^{12}	100	-	-	-	-	-		
5.10^{12}	49(1)	9.3775(9)	6.8912(8)	294(20)	0.44	0.53	24	15
10^{13}	20(1)	9.4236(5)	6.9105(5)	291(20)	0.94	0.82	9.9	6
5.10^{13}	14(1)	9.3160(4)	6.8402(5)	294(22)	-0.21	-0.22	10.5	5.9
I								
10^{11}	-	-	-	-	-	-		
5.10^{11}	86(2)	9.3603(3)	6.8790(5)	90(10)	0.26	0.35	23.9	15.1
10^{12}	-	-	-	-	-	-		
3.10^{12}	47(2)	9.3645(3)	6.8840(5)	91(6)	0.30	0.42	13.3	9
5.10^{12}	29.2(5)	9.3765(5)	6.8881(6)	77(11)	0.44	0.48	10.4	7.3
10^{13}	13.2(2)	9.3719(4)	6.8857(6)	82(9)	0.38	0.45	6.7	4.9

Single impact model associated to crystal size reduction

Cell parameters and volume increase, then relax

Amorphisation / recrystallisation competition: single or double impact

Amorphous/crystalline volume fraction (damaged fraction Fd = Va / V) as determined by x-ray diffraction

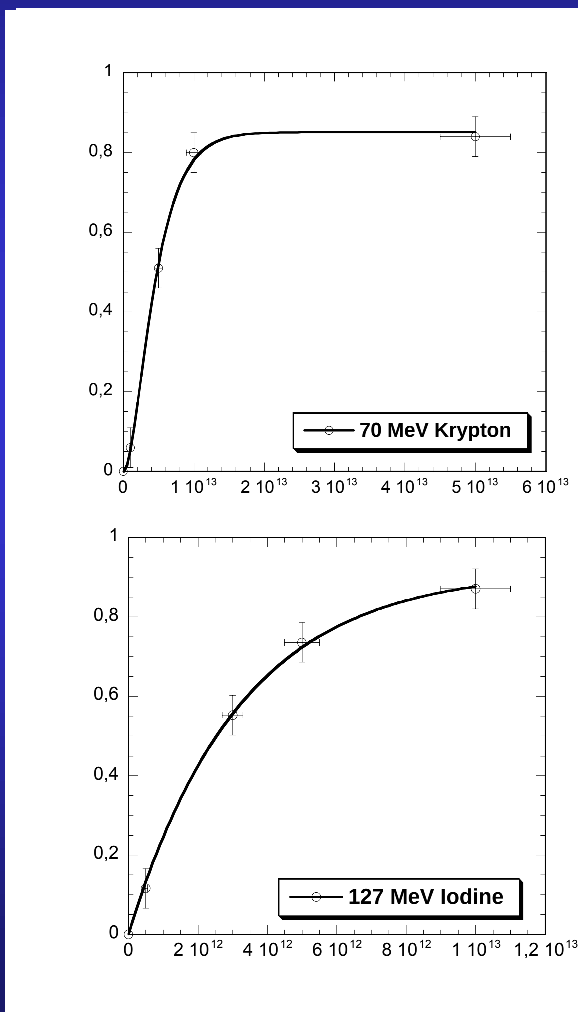

B

Fitting parameters	Krypton		Iodine
	Single impact Fd = B(1- exp(-Aϕt))	Double impact Fd = B(1 – (1+ Aϕt) exp(-Aϕt))	Single impact Fd = B(1- exp(-Aϕt))
$A = \pi R^2$ (cm^2)	$1.85 \pm 0.15\ 10^{-13}$	$4.1 \pm 0.15\ 10^{-13}$	$3.3 \pm 0.15\ 10^{-13}$
Radius R (nm)	2.4 ± 0.2	3.6	3.2
B (Max.damage rate)	0.87	0.85 ± 0.2	0.92 ± 0.2
χ2	0.013	0.0006	0.0004

Conclusions

a) Texture affects phase ratio and structure determination

b) Microstructure (crystallite size) affects texture (go to a)

c) Stresses shift peaks then affects structure and texture determination

d) Combined analysis may be a solution, unless you can destroy your sample or are not interested in macroscopic anisotropy ...

e) If you think you can destroy it, perhaps think twice

f) more information is always needed: local probes ...

g) www.ecole.ensicaen.fr/~chateign/texture/combined.pdf